ESI

Manganese 2-Phosphinophosphinine Precatalysts for Methanol/Ethanol Upgrading to Isobutanol

Daniel J. Ward,[a] Margot Marseglia,[a] Dan J. Saccomando,[b] Gary Walker[b] and Stephen M. Mansell[a,*]

a. Institute of Chemical Sciences, School of Engineering and Physical Sciences, Heriot-Watt University, Edinburgh, EH14 4AS, UK. Email: s.mansell@hw.ac.uk; Web: www.mansellresearch.org.uk.

b. Lubrizol Limited, The Knowle, Nether Lane Hazelwood, Derby, Derbyshire, DE56 4AN, UK.

1 Table of Contents

2 NMR spectra

2.1 2^{TMS}

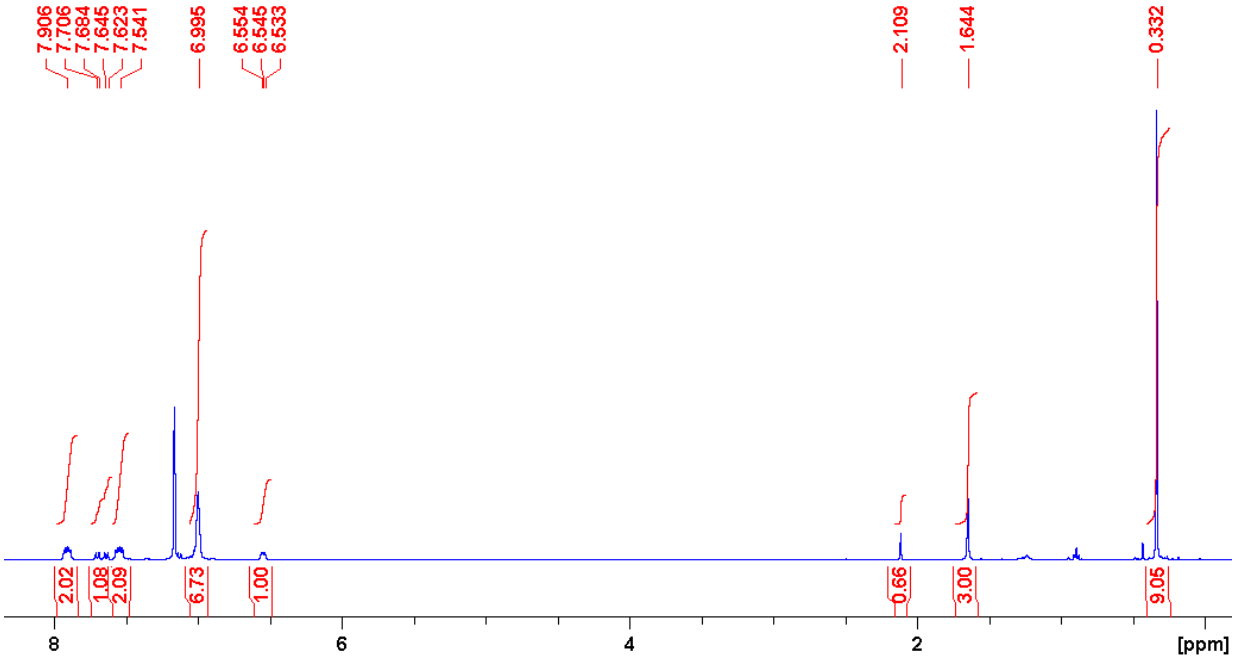

Figure S1. ^{1}H NMR spectrum (400 MHz, C_6D_6, 298 K) of $\mathbf{2^{TMS}}$; toluene solvate was observed at 2.11 ppm along with trace amounts of n-hexane.

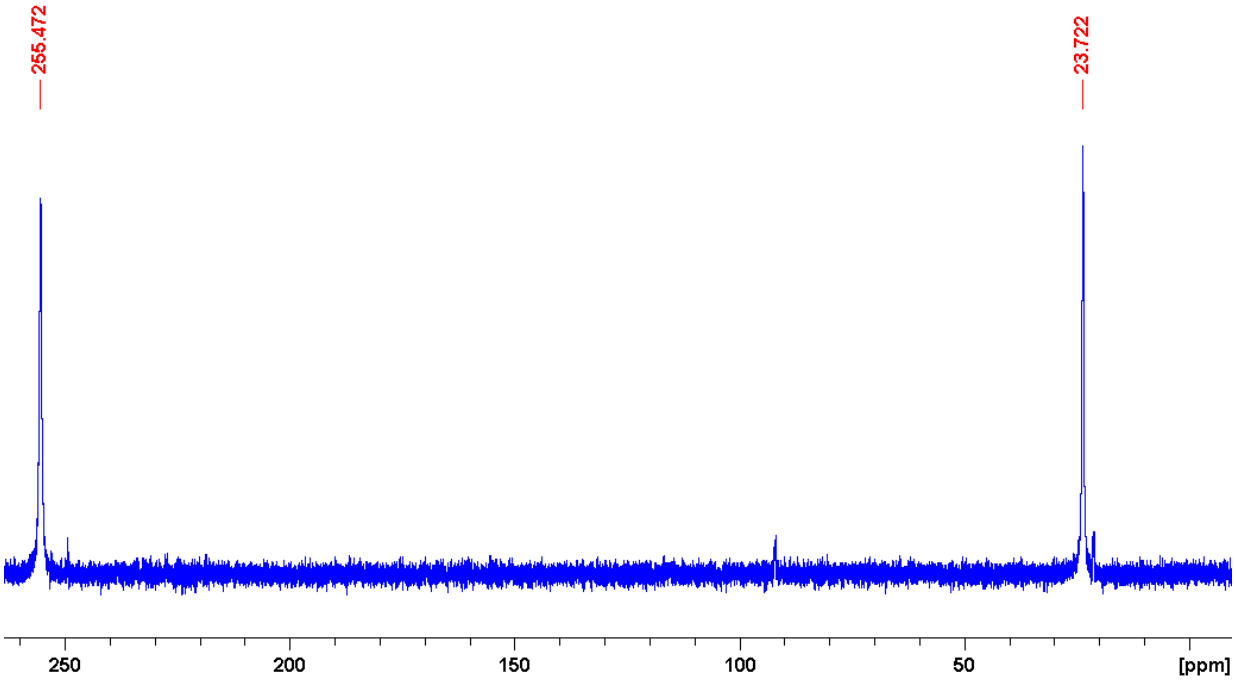

Figure S2. $^{31}P\{^{1}H\}$ NMR spectrum (162 MHz, C_6D_6, 298 K) of $\mathbf{2^{TMS}}$.

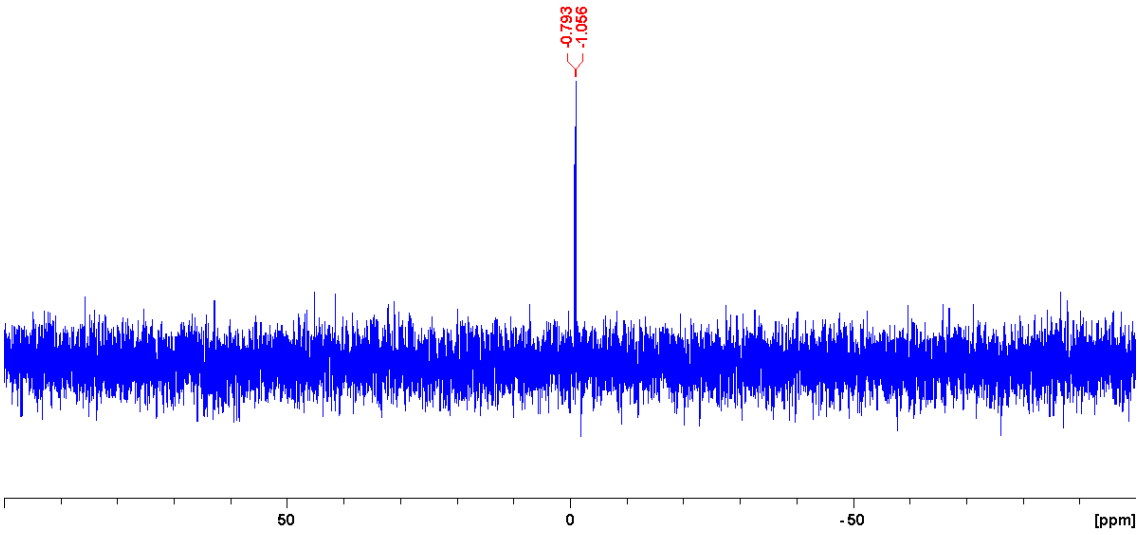

Figure S3. $^{29}Si\{^{1}H\}$ NMR spectrum (79.5 MHz, C_6D_6, 298 K) of **2**^{TMS}.

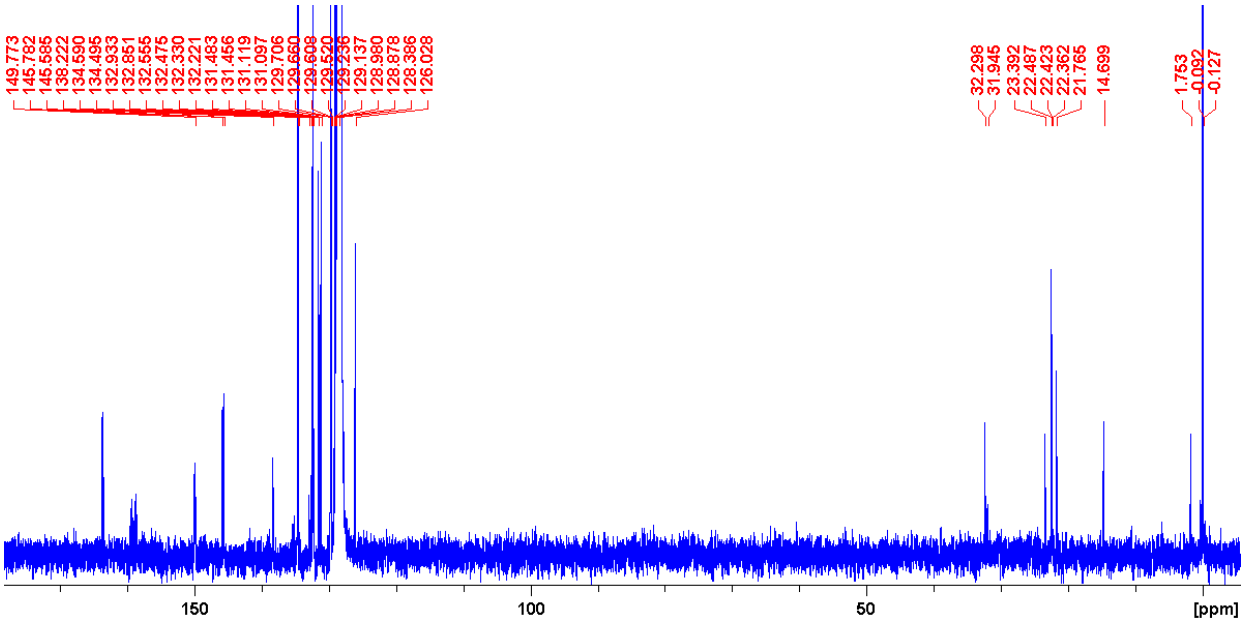

Figure S4. $^{13}C\{^{1}H\}$ NMR spectrum (101 MHz, C_6D_6, 298 K) of **2**^{TMS}.

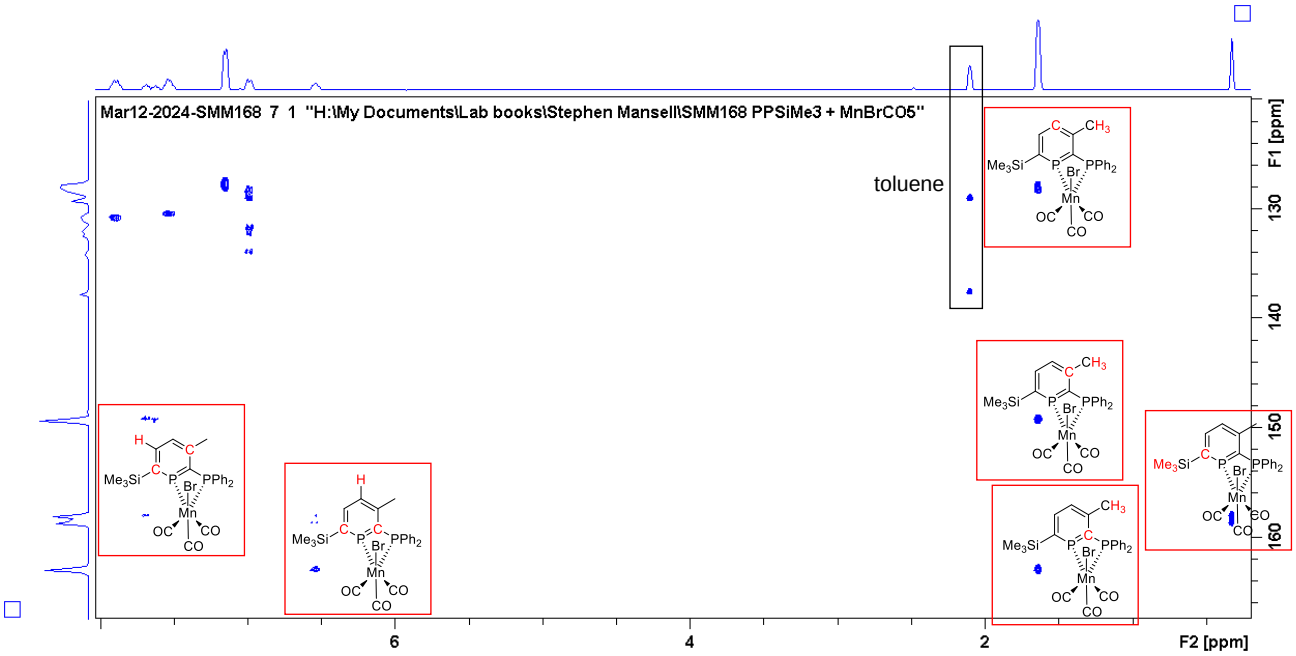

Figure S5. Key HMBC cross-peaks for **2**^{TMS}.

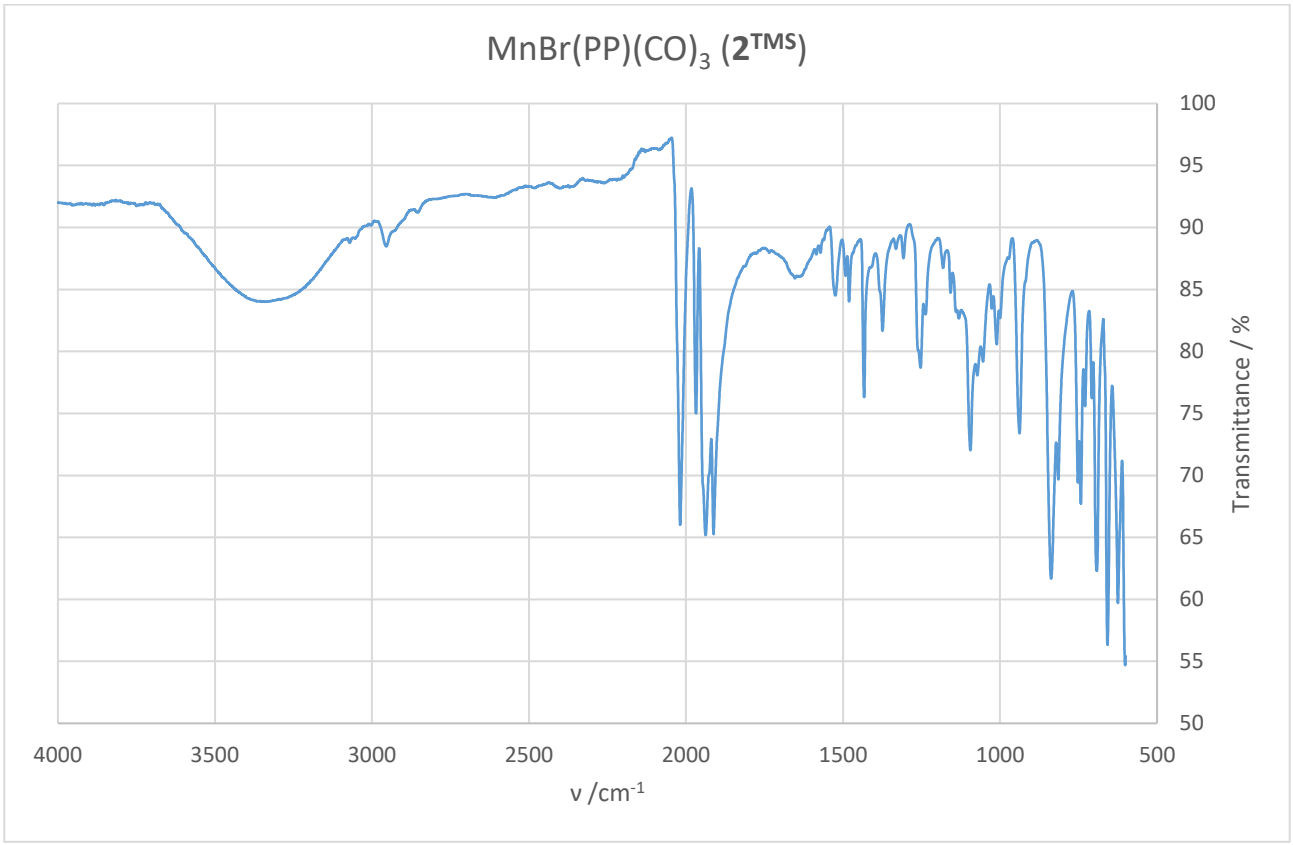

Figure S6. IR spectrum (ATR) of **2**^{TMS}.

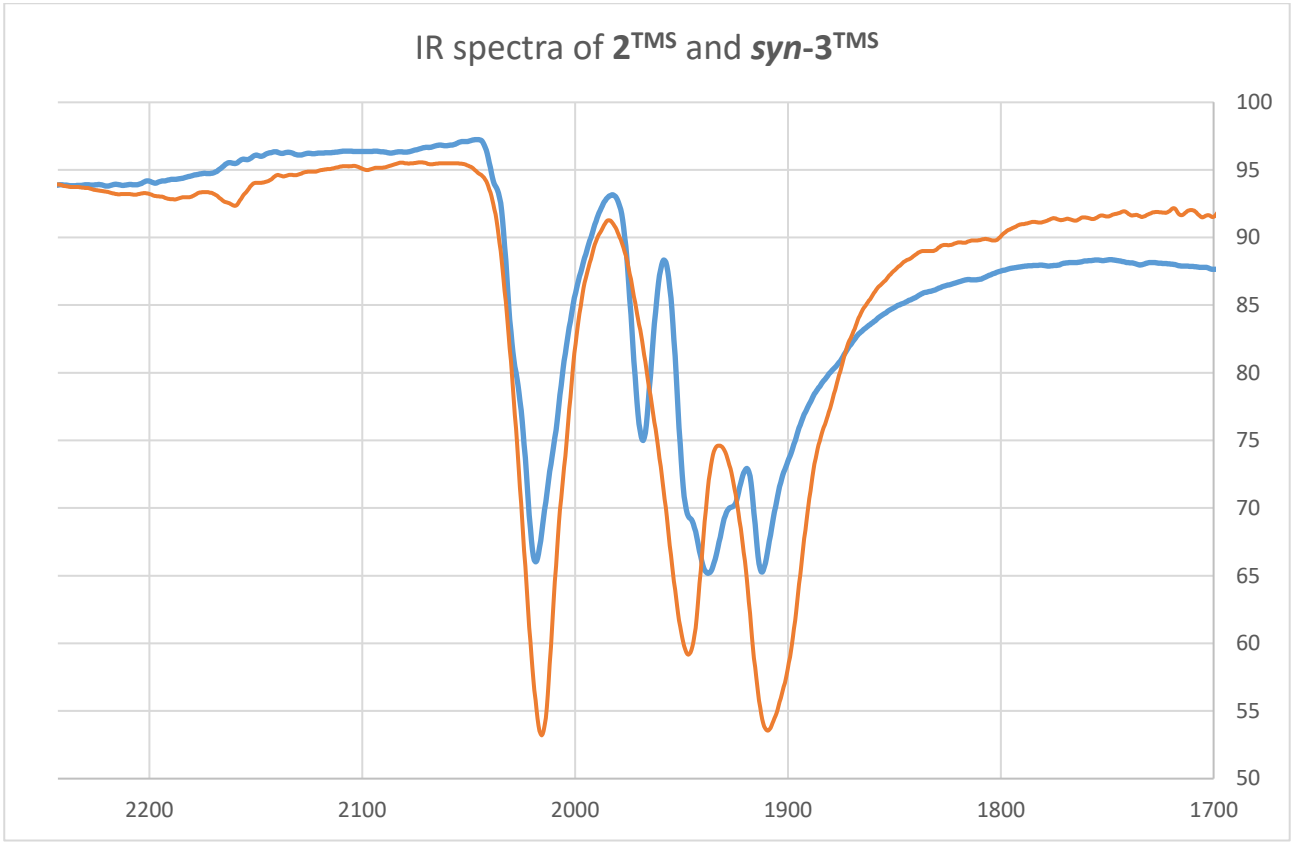

Figure S7. Comparison of carbonyl stretching frequency region for **2**^{TMS} (blue) and ***syn*-3**^{TMS} (orange).

2.2 Reactions of 2^{TMS} with H_2O

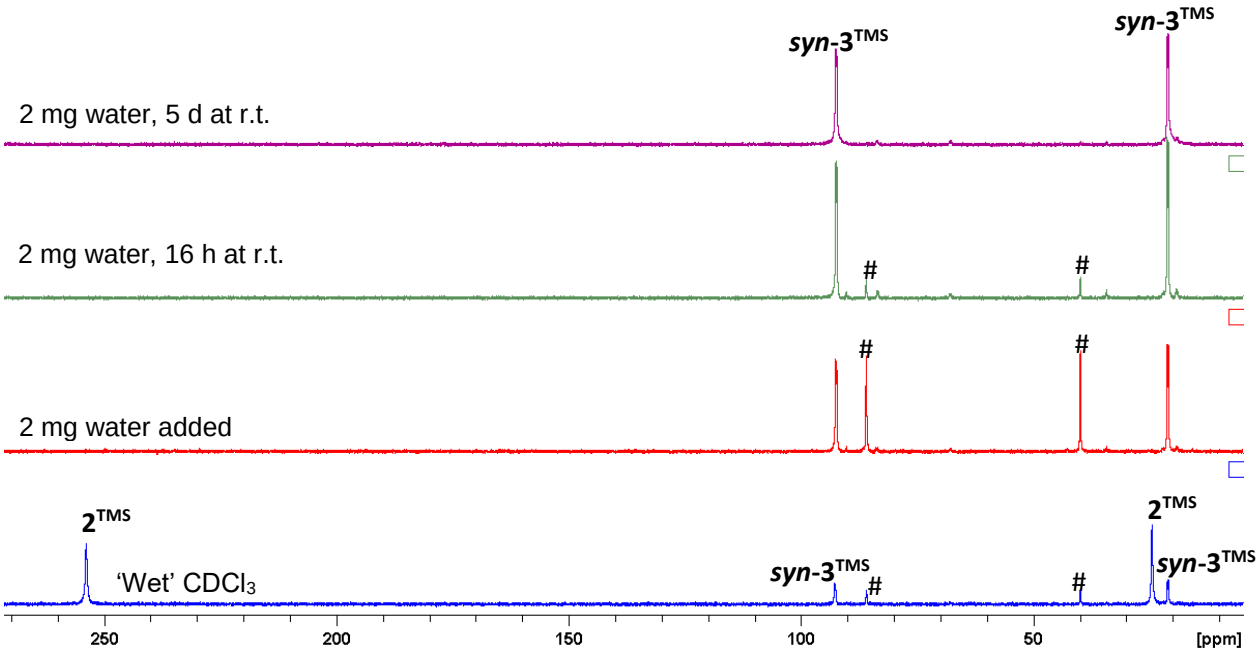

Figure S8. $^{31}P\{^1H\}$ NMR spectra (162 MHz, $CDCl_3$, 298 K) of the reaction of $\mathbf{2^{TMS}}$ with water. An intermediate was observed (#, assigned to ***1,4*-3^{TMS}**), but the reaction ultimately led cleanly to ***syn*-3^{TMS}**.

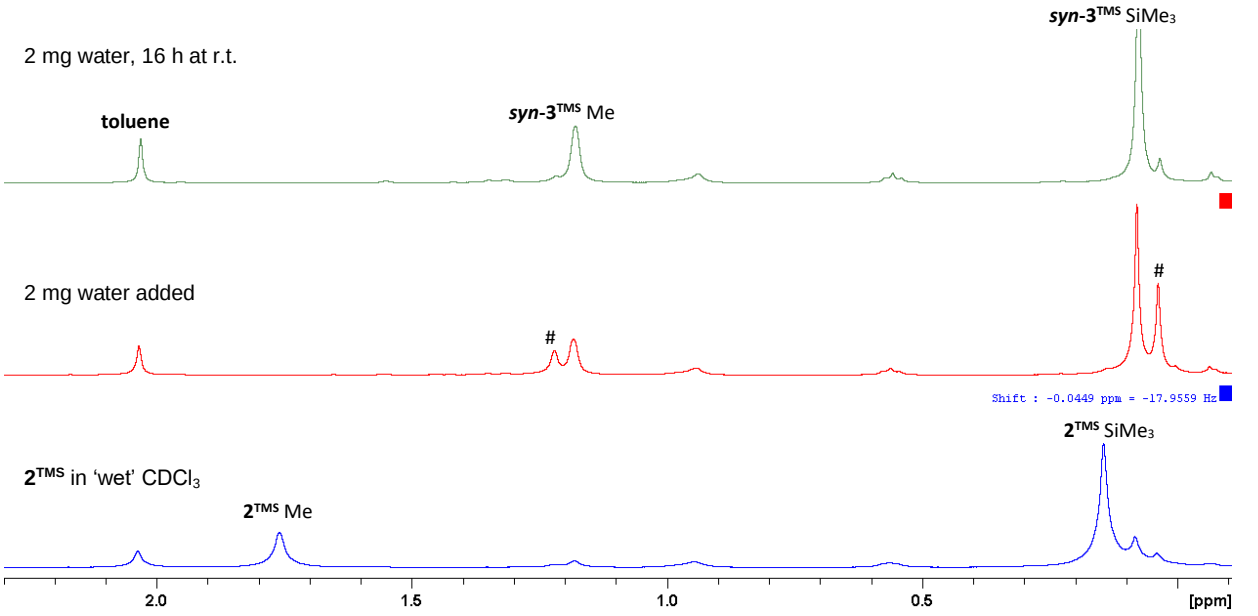

Figure S9. Alkyl region of the ^1H NMR spectra (400 MHz, $CDCl_3$, 298 K) of the reaction of $\mathbf{2^{TMS}}$ with water. An intermediate was observed (#, assigned to ***1,4*-3^{TMS}**), but the reaction ultimately led cleanly to ***syn*-3^{TMS}**.

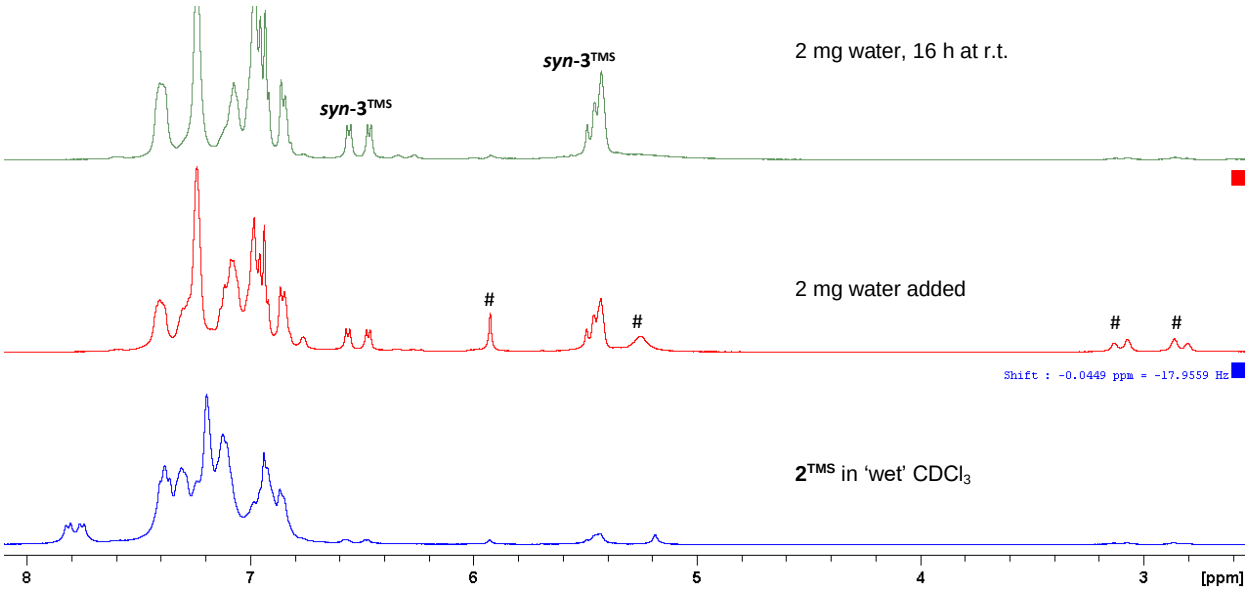

Figure S10. 8 0 – 2. 5 ppm region of the ^{1}H NMR spectra (400 MHz, $CDCl_3$, 298 K) of the reaction of **2**^{TMS} with water. An intermediate was observed (#, assigned to ***1,4*-3**^{TMS}), but the reaction ultimately led cleanly to ***syn*-3**^{TMS}.

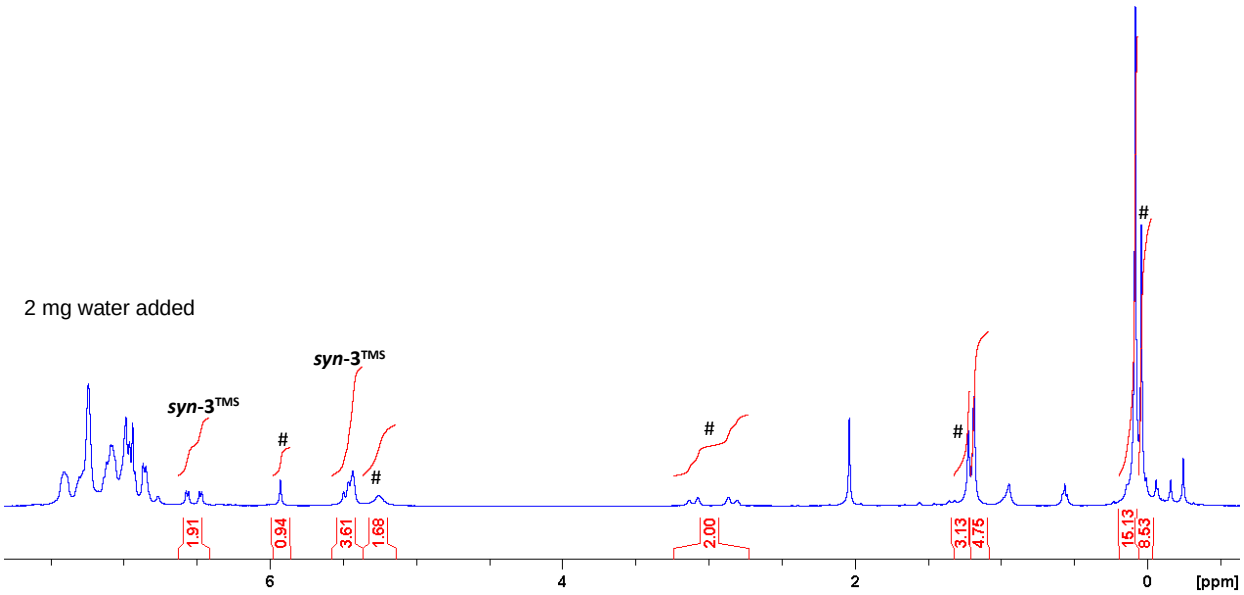

Figure S11. Integrated ^{1}H NMR spectrum (400 MHz, $CDCl_3$, 298 K) of the mixture resulting from **2**^{TMS} + 2 mg of water. ^{31}P{^{1}H} NMR spectroscopy gave an approximate ratio of 2:1 ***syn*-3**^{TMS} : additional isomer (#, assigned to ***1,4*-3**^{TMS}) at this stage of the reaction, in reasonable agreement with the integrations here. Key evidence for the formation of ***1,4*-3**^{TMS} are the mutually coupled doublets integrating to one proton each at ca. 3 ppm.

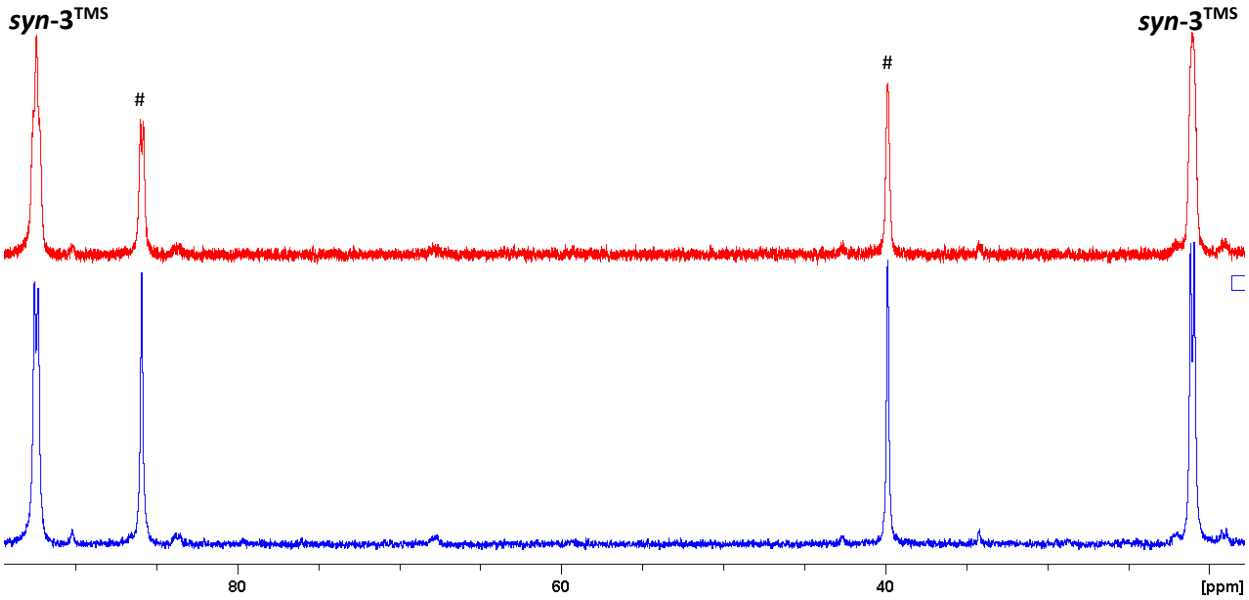

Figure S12. ^{31}P NMR (top) and $^{31}P\{^{1}H\}$ NMR (bottom) spectra (162 MHz, $CDCl_3$, 298 K) of the reaction of $\mathbf{2^{TMS}}$ with water. No coupling to the PPh_2 indicated by # is evident, in agreement with the assignment as ***1,4*-3^{TMS}**.

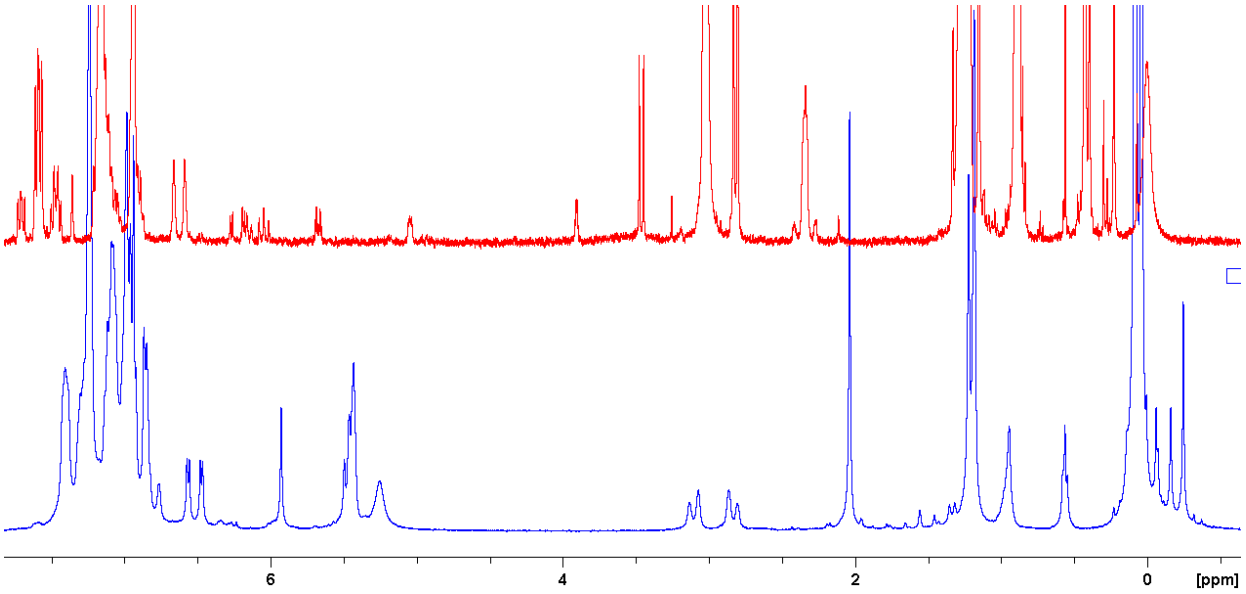

Figure S13. Comparison of ^{1}H NMR spectra (400 MHz, $CDCl_3$, 298 K) for ***1,4*-4^{TMS}** (and two other isomers as impurities; top, red spectrum) with ***syn*-3^{TMS}** and additional isomer (bottom, blue spectrum) assigned as ***1,4*-3^{TMS}**.

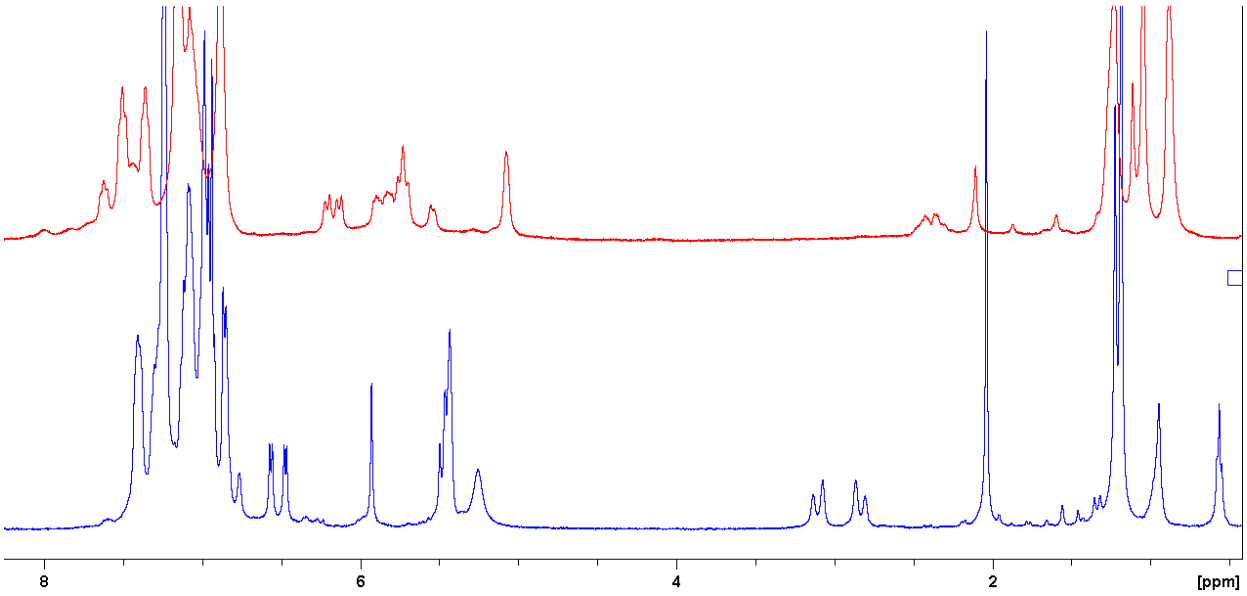

Figure S14. Comparison of ^{1}H NMR spectra (400 MHz, $CDCl_3$, 298 K) for ***2***^{H} + water (top red spectrum) with ***2***^{TMS} + water (bottom, blue spectrum).

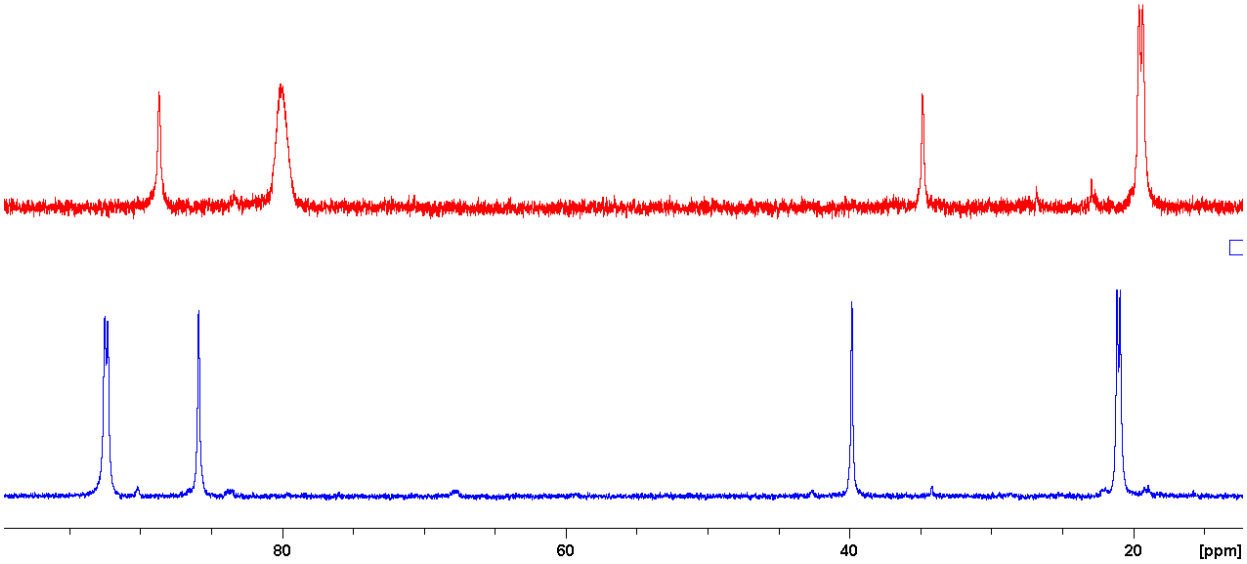

Figure S15. Comparison of $^{31}P\{^{1}H\}$ NMR spectra (162 MHz, 298 K) for ***2***^{H} + water (C_6D_6, top red spectrum) with ***2***^{TMS} + water ($CDCl_3$, bottom, blue spectrum).

2.3 *syn*-3^{TMS}

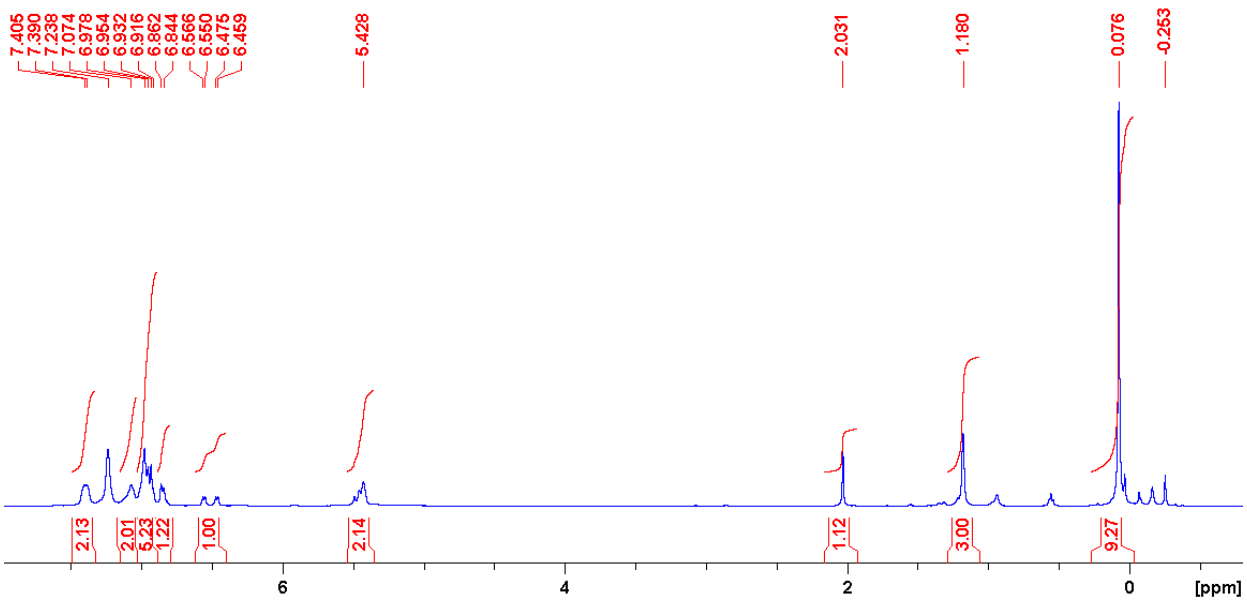

Figure S16. ^{1}H NMR spectrum (400 MHz, C_6D_6, 298 K) of ***syn*-3^{TMS}**; trace amounts of toluene and n-hexane present.

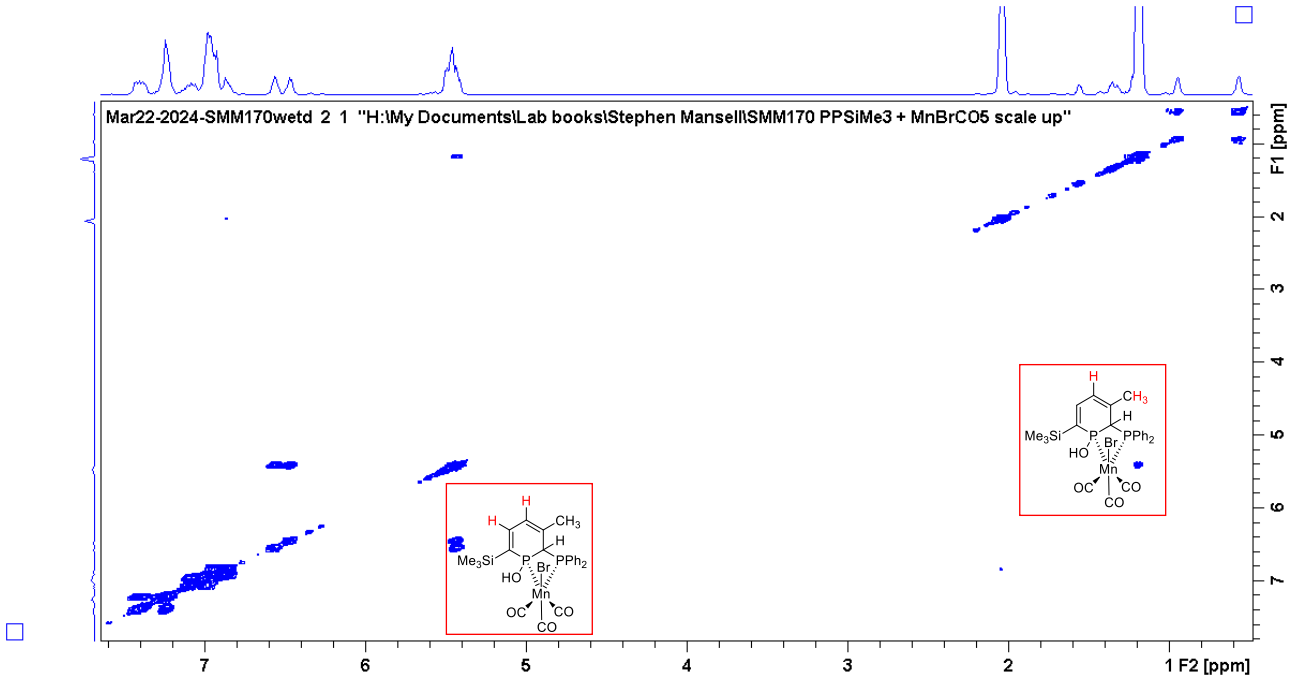

Figure S17. ^{1}H-^{1}H COSY for ***syn*-3^{TMS}**.

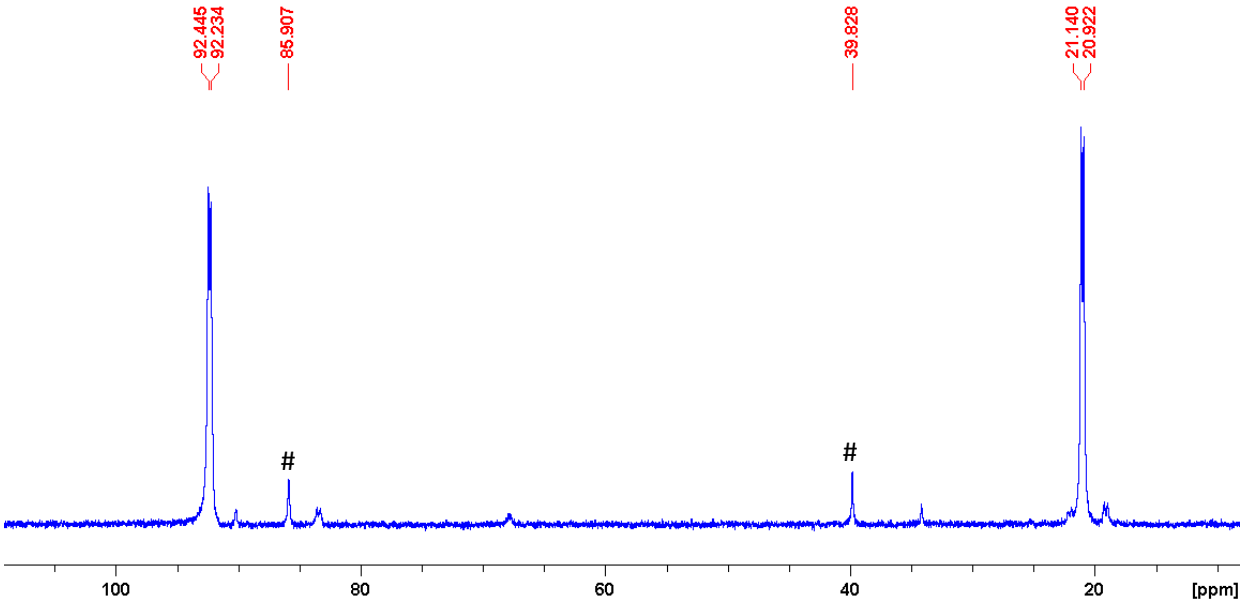

Figure S18. $^{31}P\{^{1}H\}$ NMR spectrum (162 MHz, C_6D_6, 298 K) of ***syn*-3^{TMS}**. Intermediate (#, assigned to ***1,4*-3^{TMS}**) observed at 85.9 and 39.8 ppm.

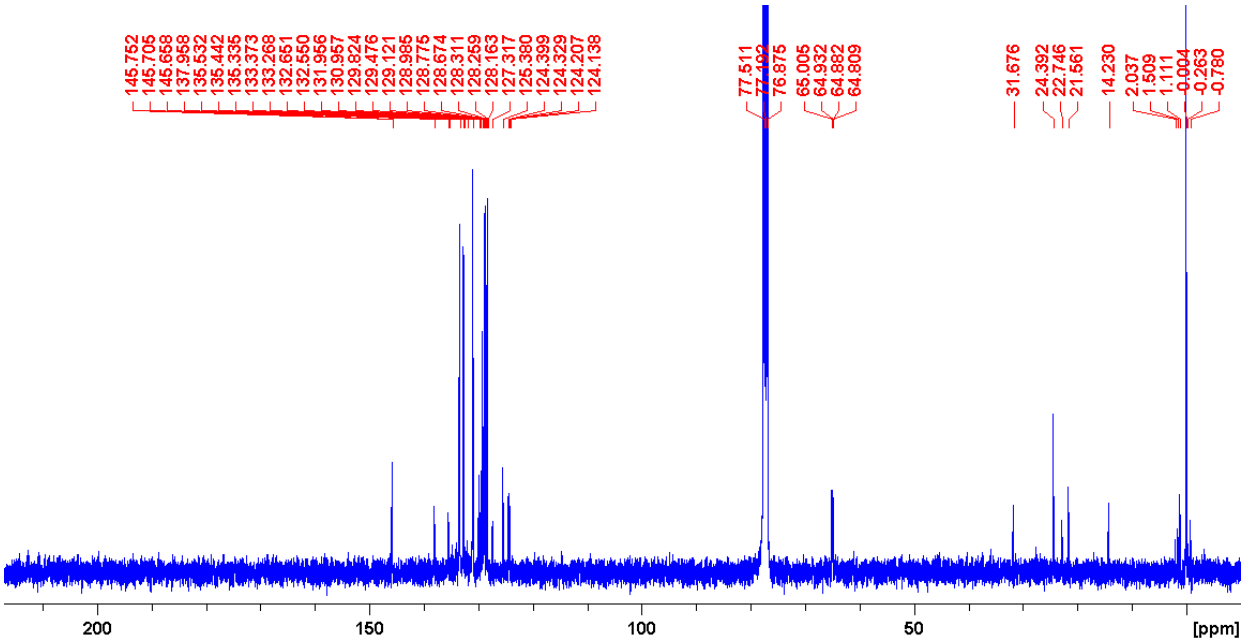

Figure S19. $^{13}C\{^{1}H\}$ NMR spectrum (101 MHz, C_6D_6, 298 K) of ***syn*-3^{TMS}**. Trace impurities of toluene and n-hexane were also observed.

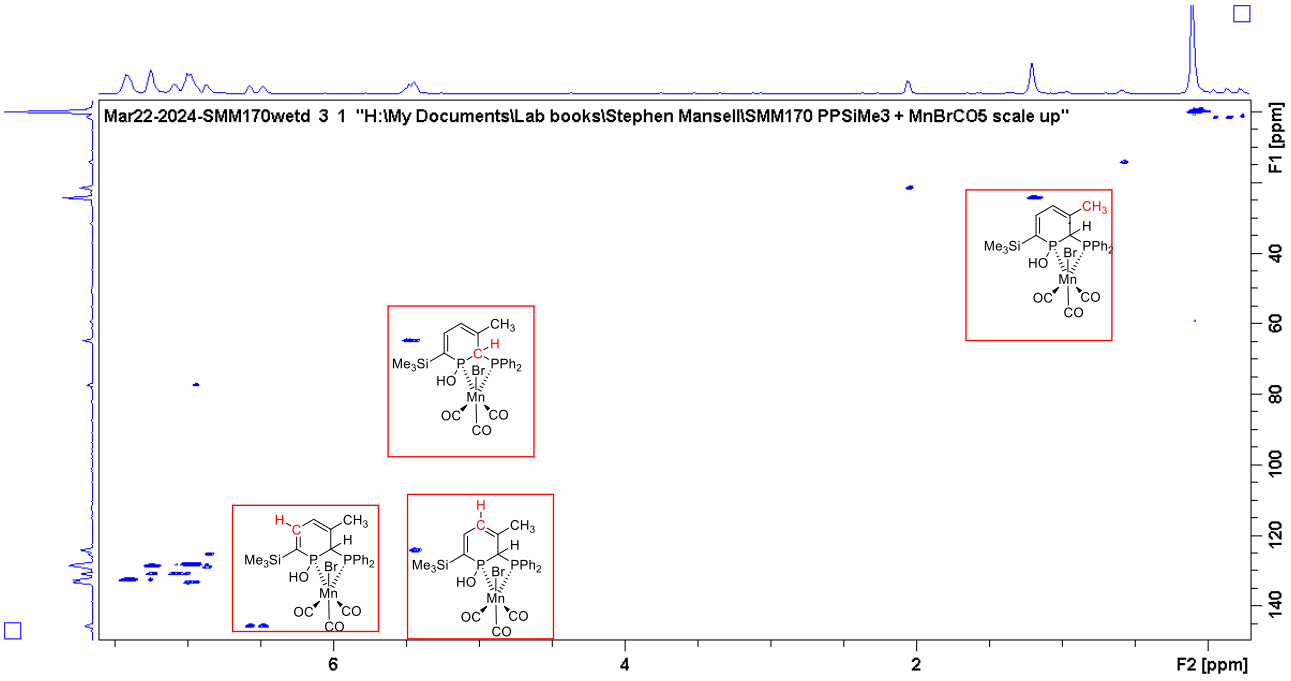

Figure S20. HSQC for ***syn*-3^{TMS}**.

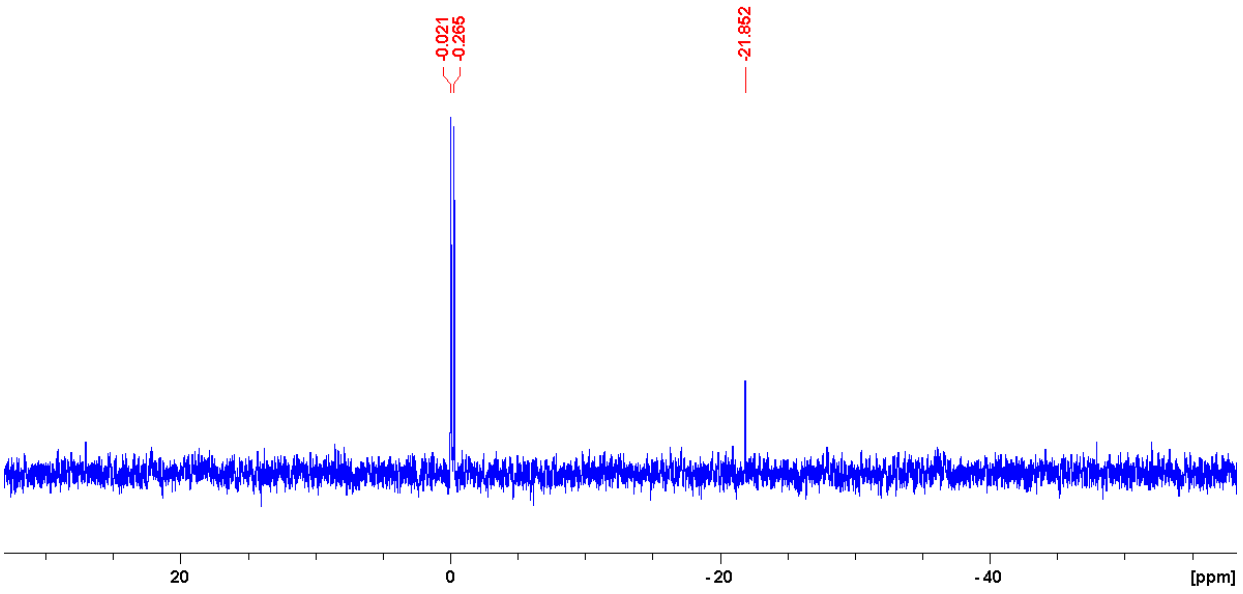

Figure S21. $^{29}Si\{^{1}H\}$ NMR spectrum (79.5 MHz, C_6D_6, 298 K) of ***syn*-3^{TMS}**. Resonance at -21.9 ppm is silicone grease as a trace impurity.

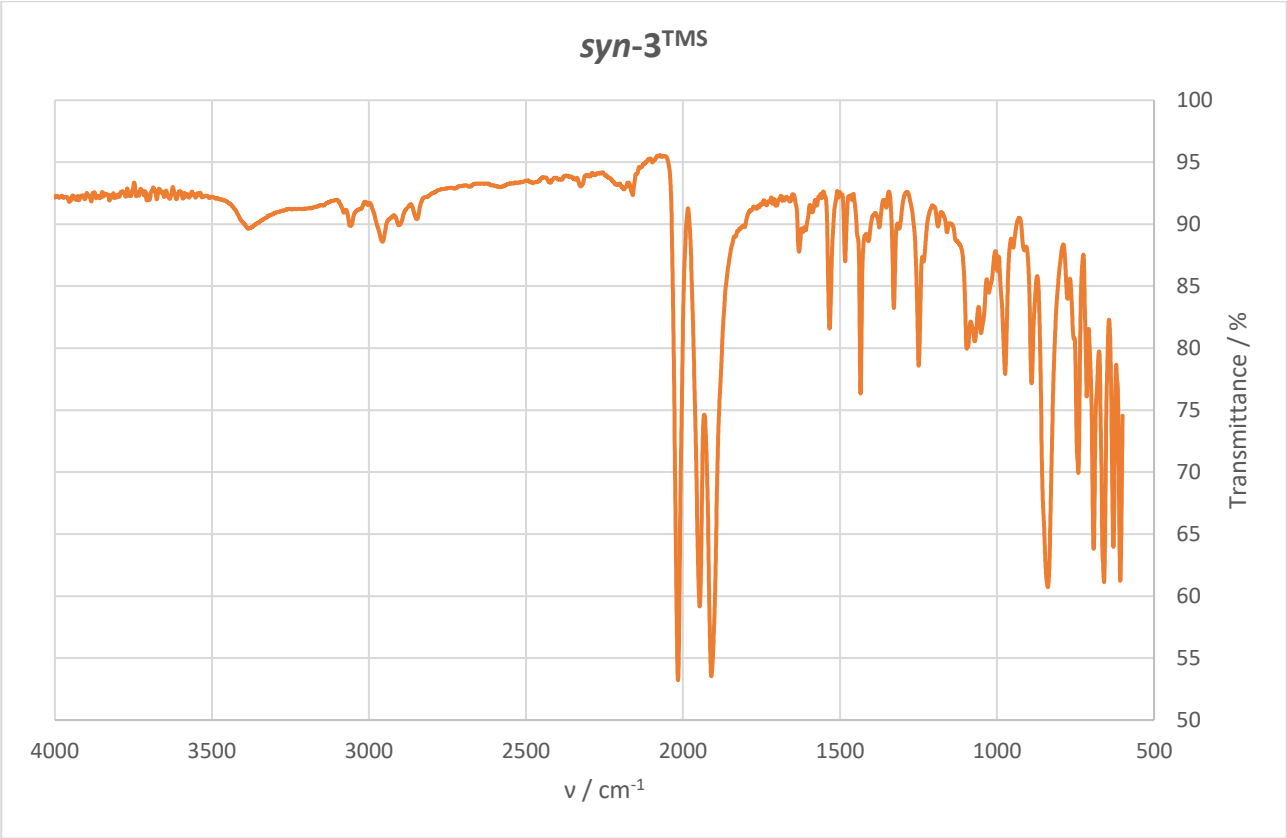

Figure S22. IR spectrum (ATR) of ***syn*-3^{TMS}**.

2.4 Reactions of 2^{TMS} with MeOH

Reaction with dry MeOH revealed that multiple products formed. Four diphosphorus compounds in an approximate ratio of 1:1:2:4.2 was observed by $^{31}P\{^{1}H\}$ NMR spectroscopy at this concentration.

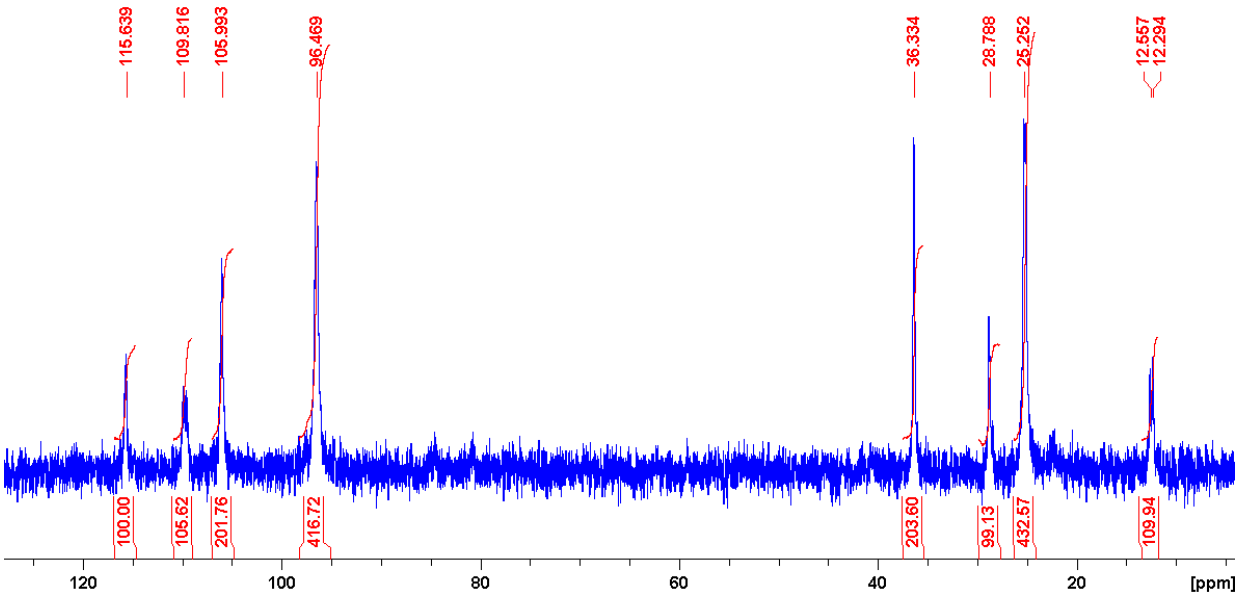

Figure S23. $^{31}P\{^{1}H\}$ NMR spectrum (162 MHz, C_6D_6, 298 K) of the reaction of $\mathbf{2^{TMS}}$ with dry MeOH.

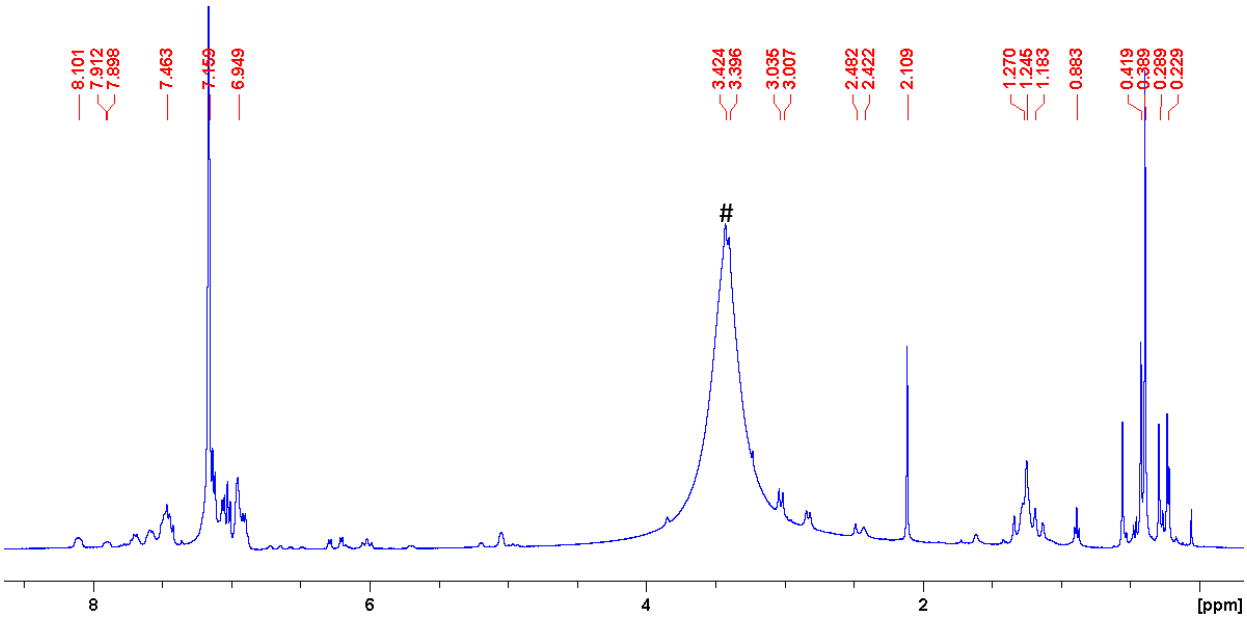

Figure S24. ^{1}H NMR spectrum (400 MHz, C_6D_6, 298 K) of the reaction of $\mathbf{2^{TMS}}$ with dry MeOH (excess, denoted by #).

Repetition of 2^{TMS} + dry MeOH on a larger scale and at a higher concentration of metal complex:

Five diphosphorus complexes are now evident.

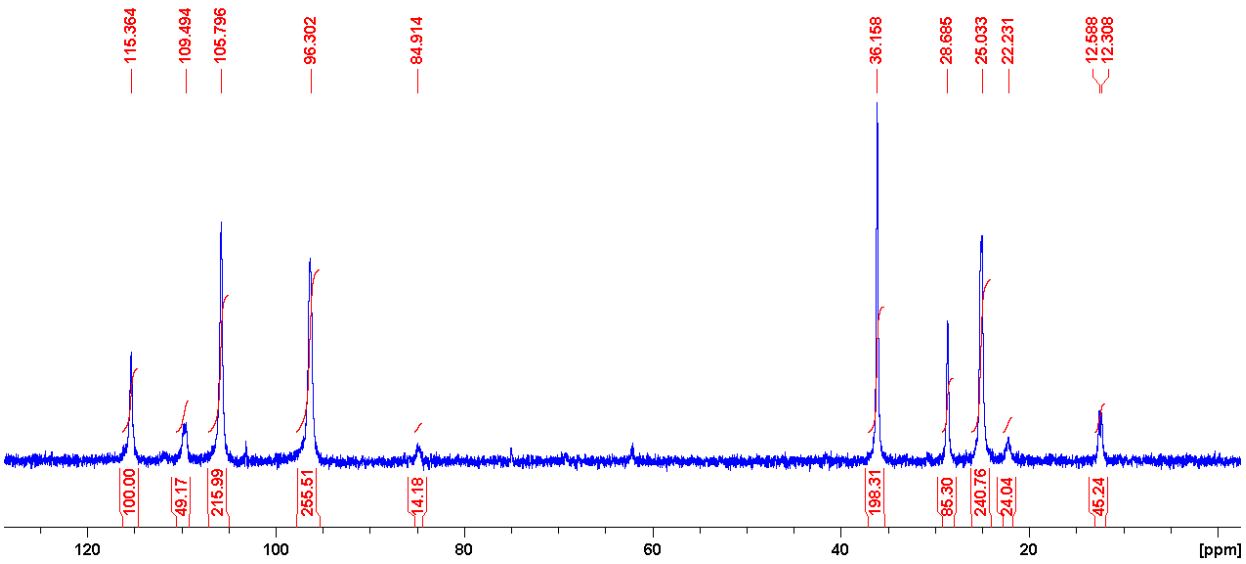

Figure S25. $^{31}P\{^{1}H\}$ NMR spectrum (162 MHz, C_6D_6, 298 K) of the reaction of $\mathbf{2^{TMS}}$ with dry MeOH.

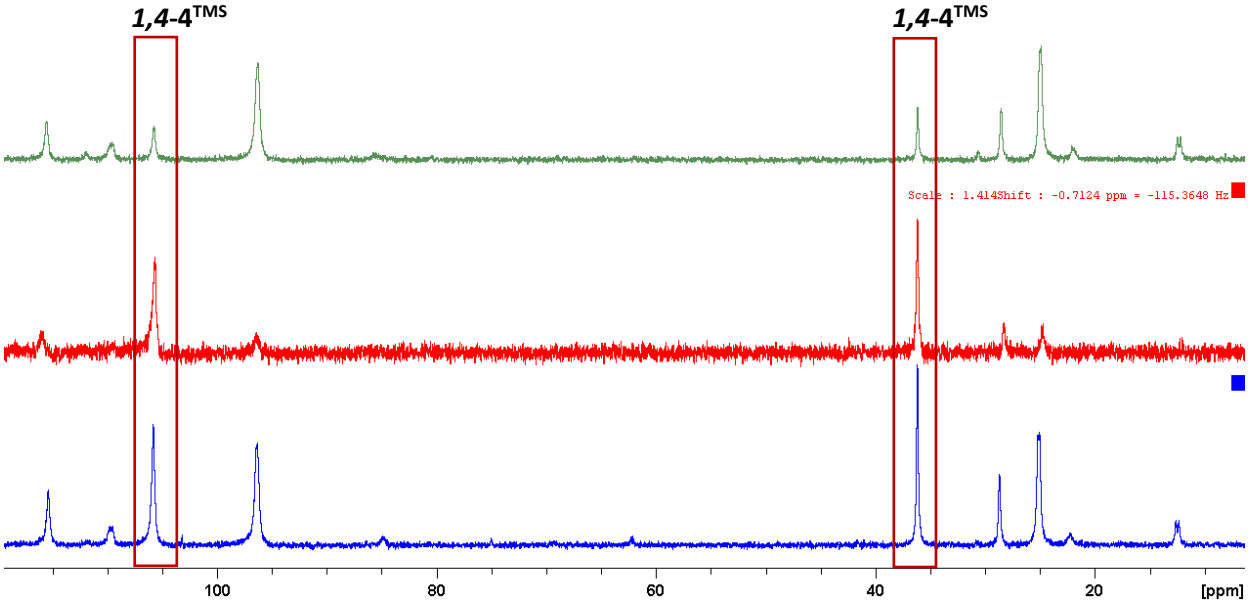

Figure S26. $^{31}P\{^{1}H\}$ NMR spectra (162 MHz, C_6D_6, 298 K) from the repetition of the reaction of $\mathbf{2^{TMS}}$ with dry MeOH. Blue: spectrum after 10 mins showing five isomers; red: isolated crystals of ***1,4*-4^{TMS}**; green: supernatant solution left after crystallisation of ***1,4*-4^{TMS}** showing a decrease in intensity of resonances for ***1,4*-4^{TMS}**.

***1,4*-4^{TMS}**

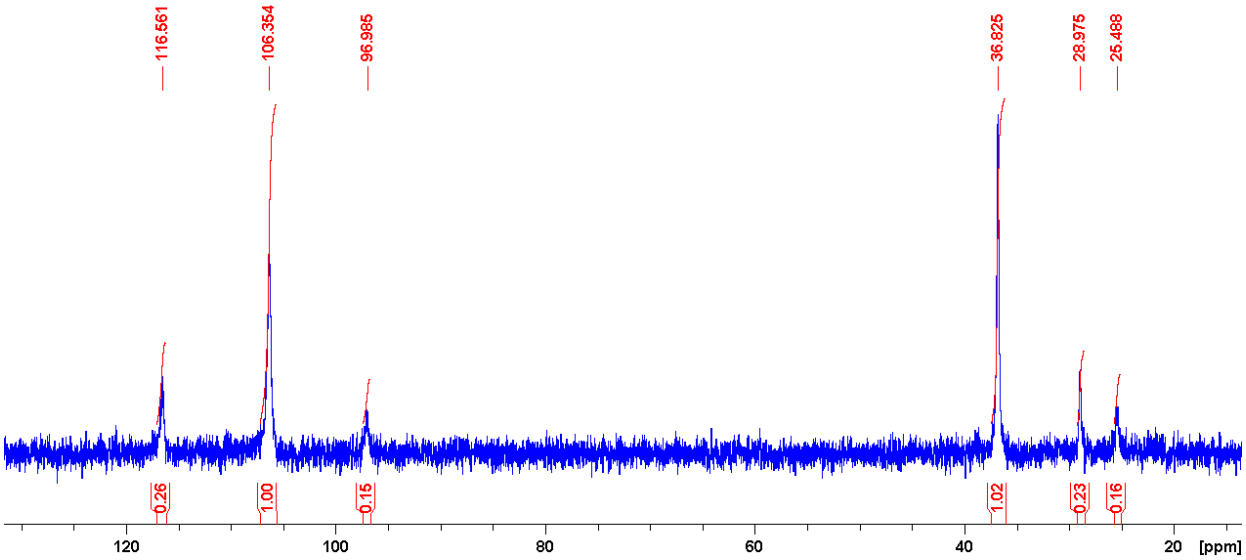

Figure S27. $^{31}P\{^{1}H\}$ NMR spectrum (162 MHz, C_6D_6, 298 K) of isolated crystals of ***1,4*-4^{TMS}** that were redissolved in C_6D_6. Impurities in the form of small amounts of two other isomers are evident.

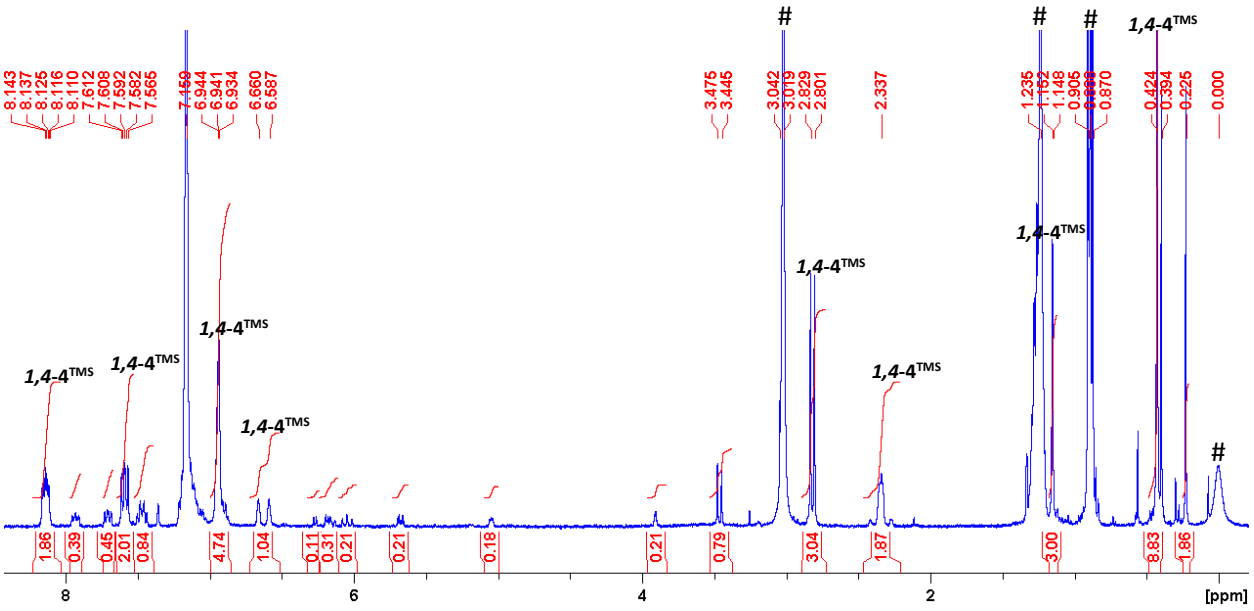

Figure S28. ^{1}H NMR spectrum (400 MHz, C_6D_6, 298 K) of redissolved crystals of ***1,4*-4^{TMS}**. Residual MeOH is at 3.04 ppm (CH_3) and 0.0 ppm (OH), and n-hexane is at 0.89 and 1.2 ppm (solvent indicated with #).

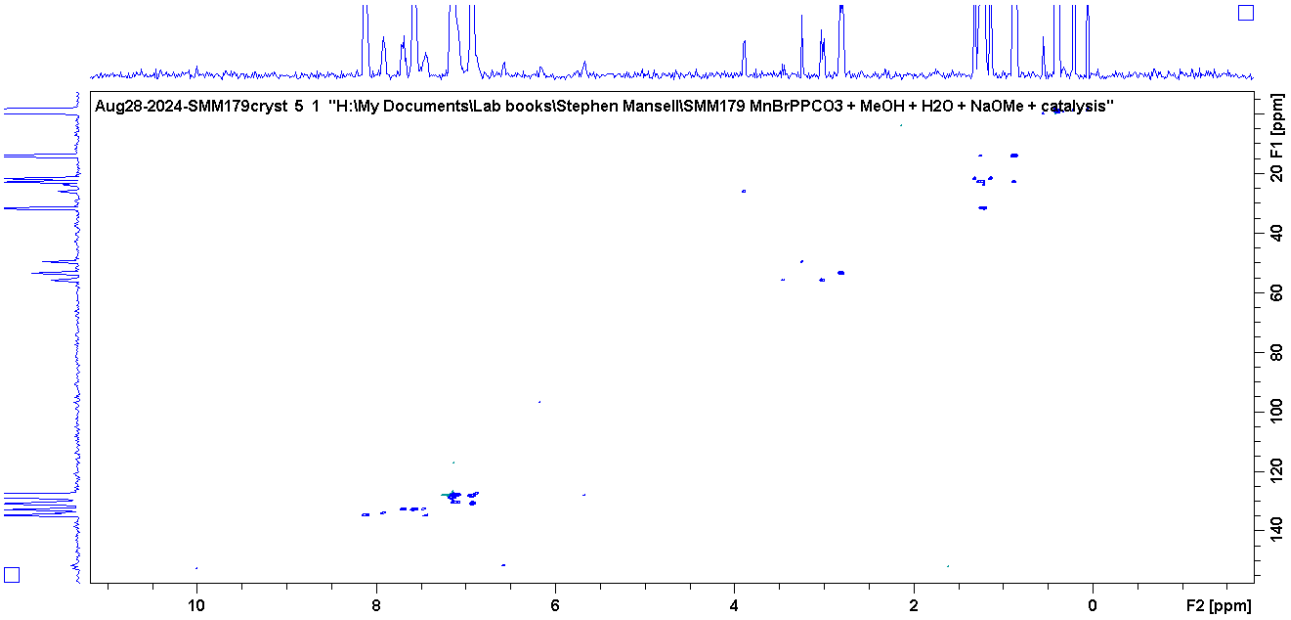

Figure S29. HSQC NMR spectrum (400 MHz, C_6D_6, 298 K) of ***1,4*-4^{TMS}**.

Reactions of MeOH addition products with water:

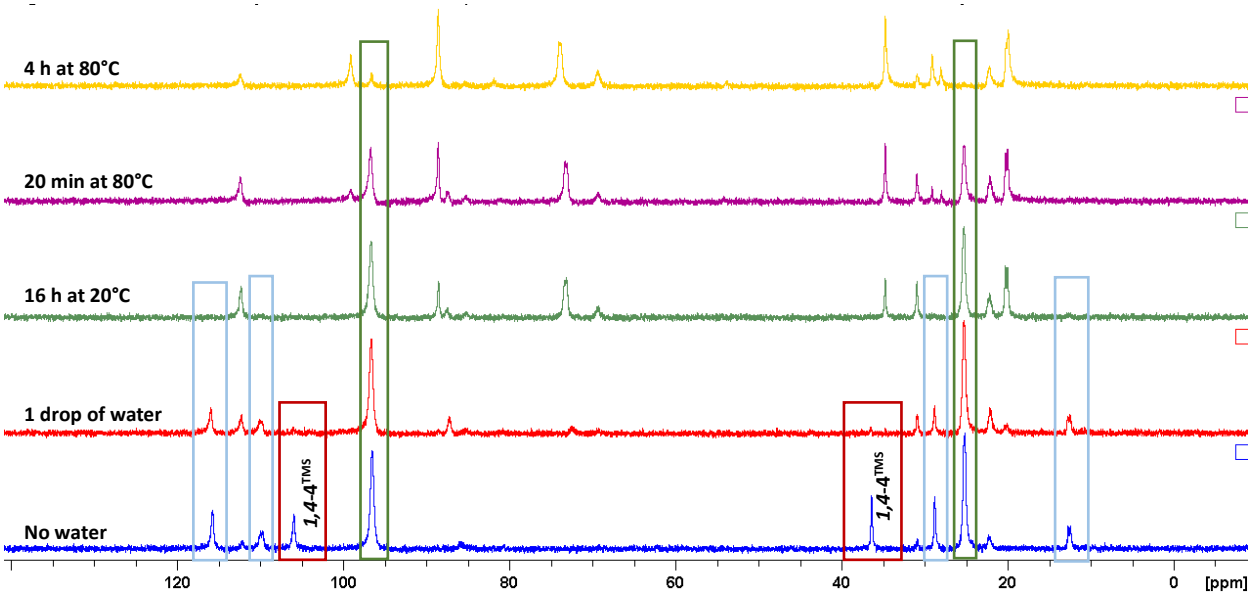

Figure S30. $^{31}P\{^{1}H\}$ NMR spectra (162 MHz, C_6D_6, 298 K) from the reaction of ***1,4*-4^{TMS}** (in red boxes) and other MeOH addition products with water. Isomers that reacted over several hours at room temperature are shown in blue boxes, and the slowest isomer to react is shown in a green box.

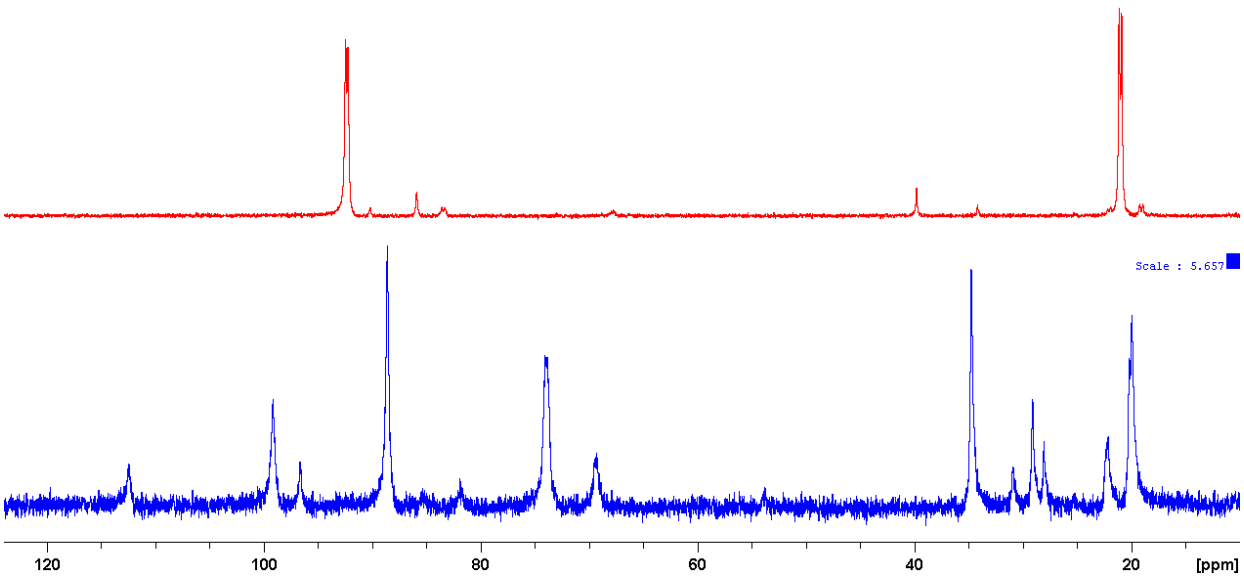

Figure S31. $^{31}P\{^{1}H\}$ NMR spectra (162 MHz, C_6D_6, 298 K) comparing the products resulting from the reaction of ***1,4*-4^{TMS}** and other MeOH addition products with water (blue) with ***syn*-3^{TMS}** (red).

2.5 2^{H}

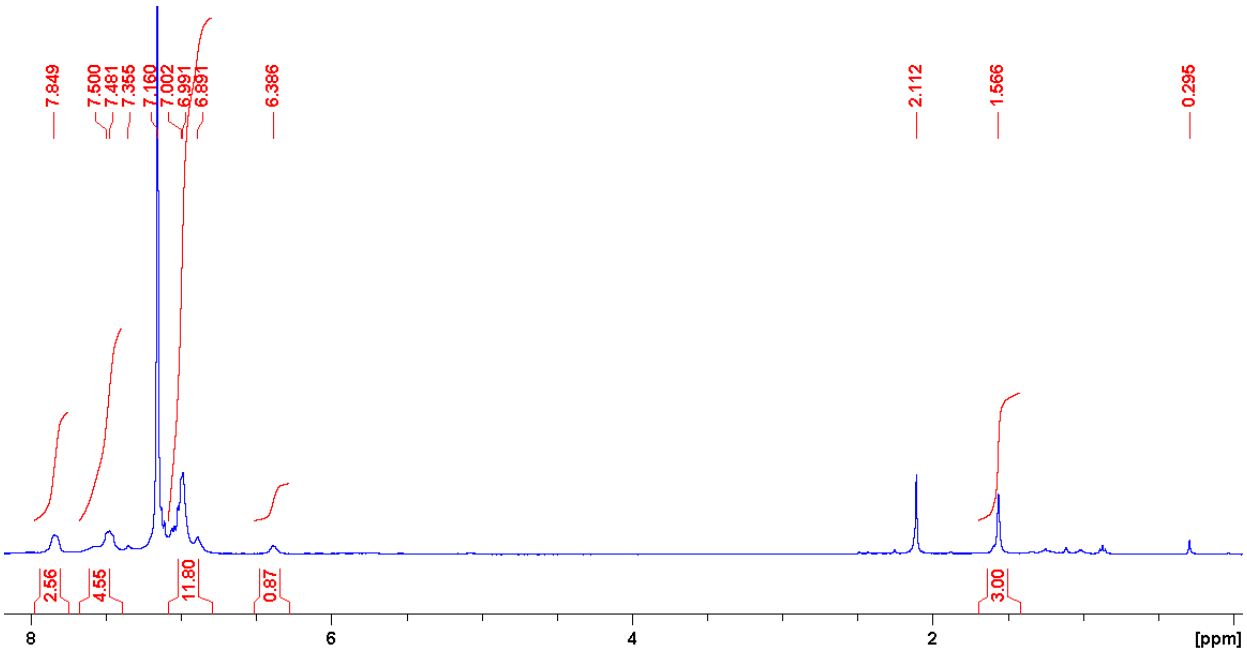

Figure S32. ^{1}H NMR spectrum (400 MHz, C_6D_6, 298 K) of $\mathbf{2^{H}}$; toluene solvent was observed at 2.11 ppm along with trace amounts of n-pentane.

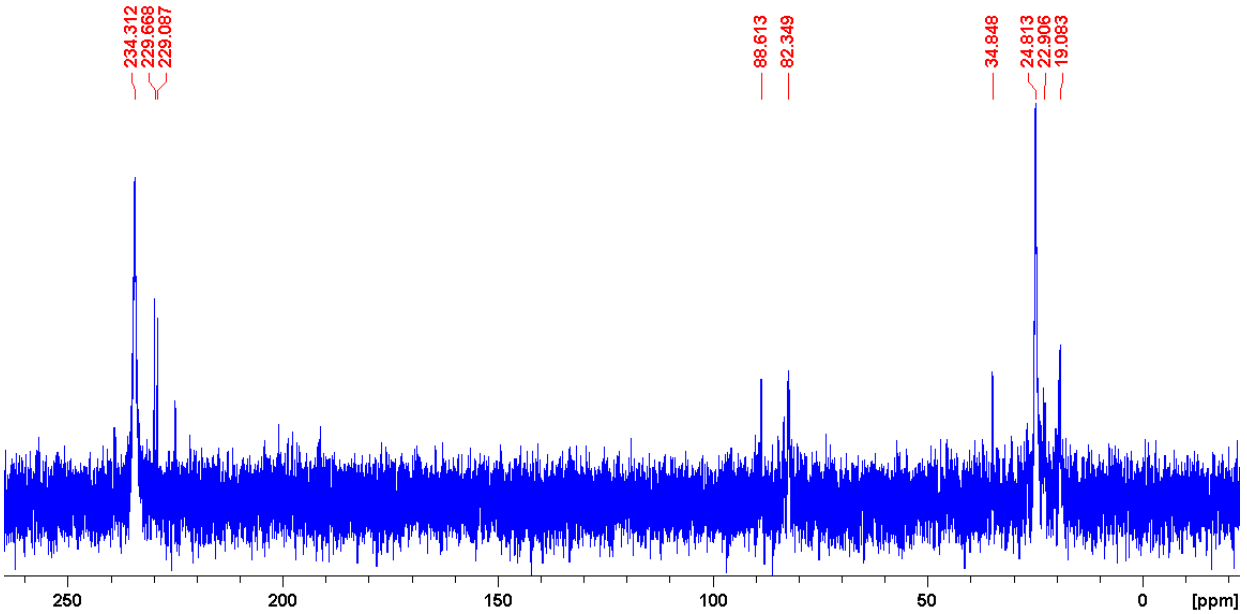

Figure S33. $^{31}P\{^{1}H\}$ NMR spectrum (162 MHz, C_6D_6, 298 K) of $\mathbf{2^{H}}$. Traces of hydrolysed $\mathbf{3^{H}}$ were observed at 89, 82, 35 and 19 ppm indicating a high degree of moisture sensitivity.

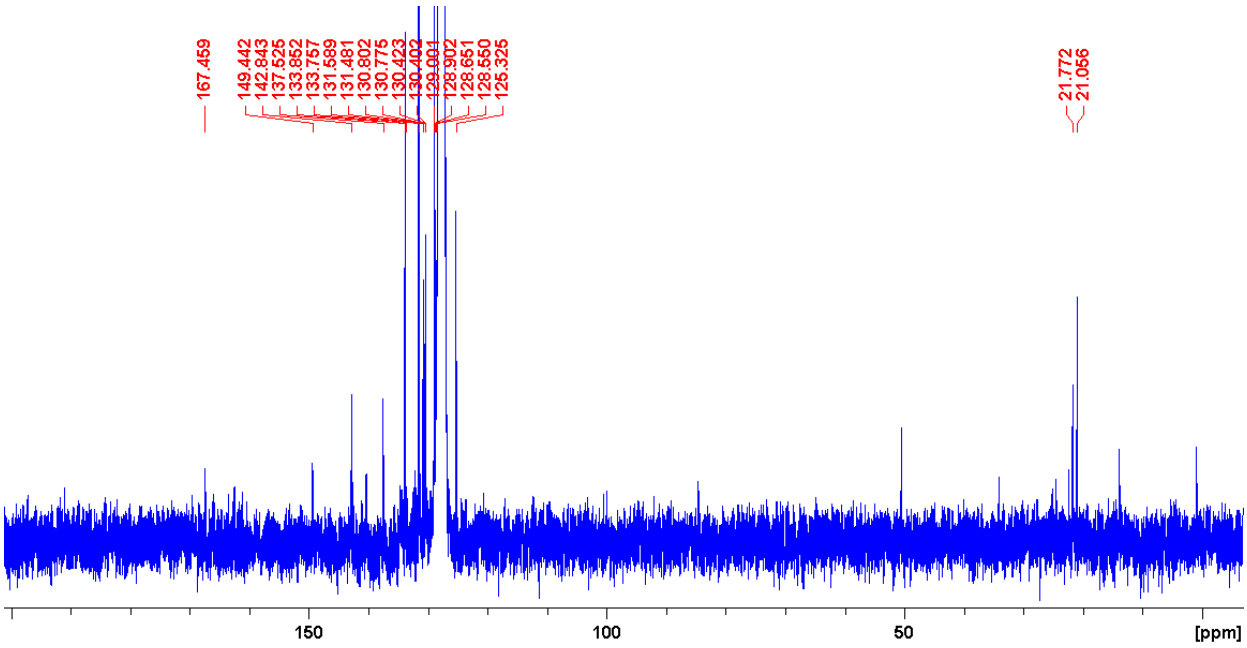

Figure S34. $^{13}C\{^{1}H\}$ NMR spectrum (101 MHz, C_6D_6, 298 K) of **2^{H}**

2.6 Reactions of 2^{H} with water

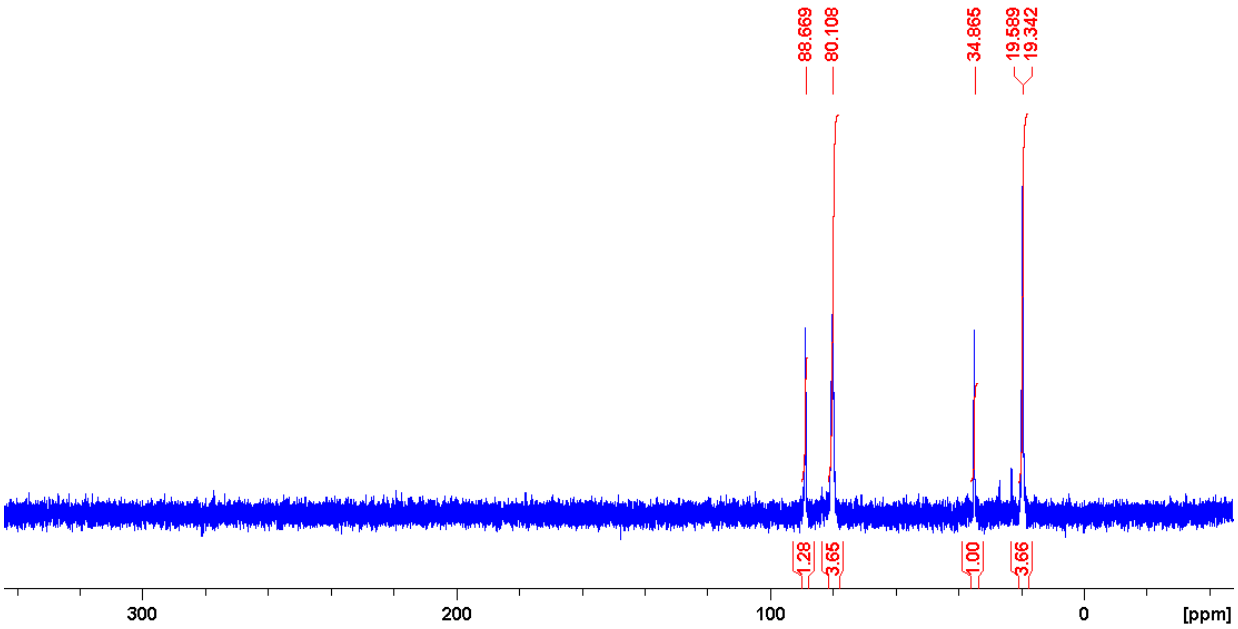

Figure S35. $^{31}P\{^{1}H\}$ NMR spectrum (162 MHz, C_6D_6, 298 K) of the reaction of **2^{H}** with H_2O.

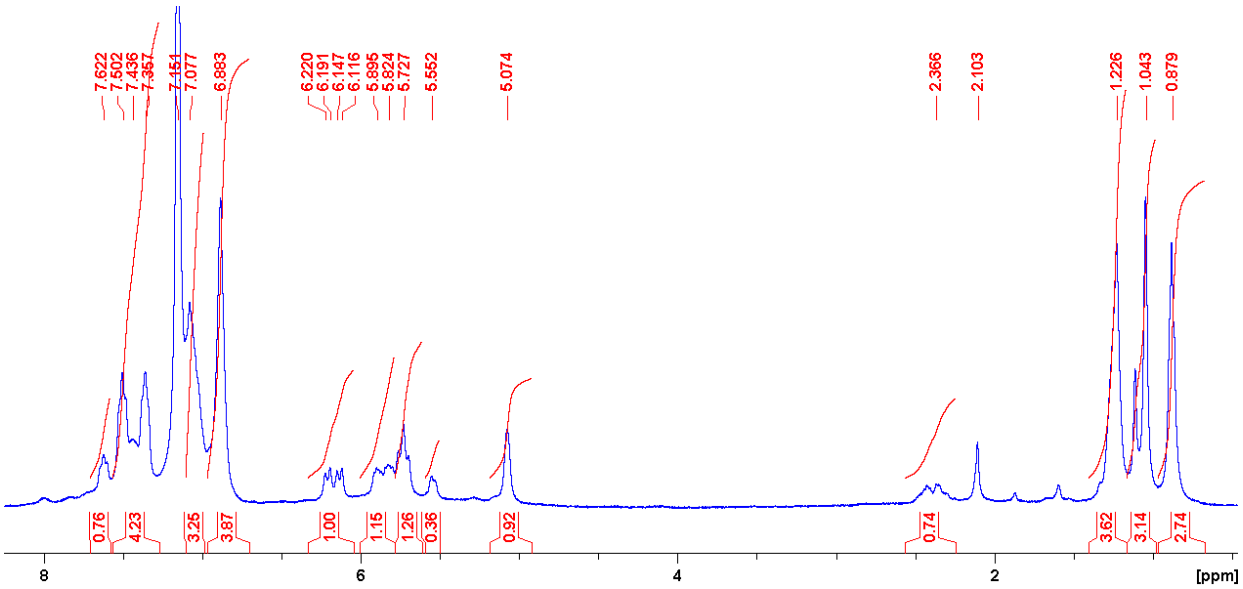

Figure S36. ^{1}H NMR spectrum (400 MHz, C_6D_6, 298 K) of the reaction of **2^{H}** with H_2O.

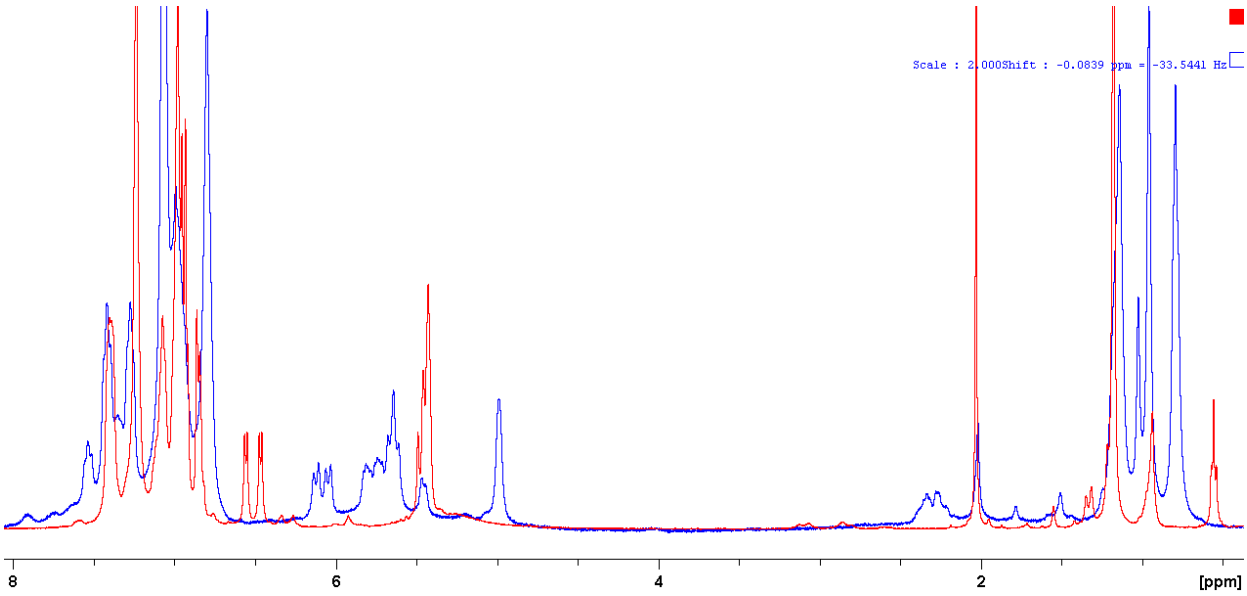

Figure S37. ^{1}H NMR spectra (400 MHz, 298 K) comparing ***syn*-3^{TMS}** (red, $CDCl_3$) with the reaction of **2^{H}** (blue, C_6D_6) with H_2O.

2.7 Reactions of 2^H with MeOH

Reaction with dry MeOH revealed that multiple products formed. The signal-to-noise ratio is poorer, and some free ligand is present.

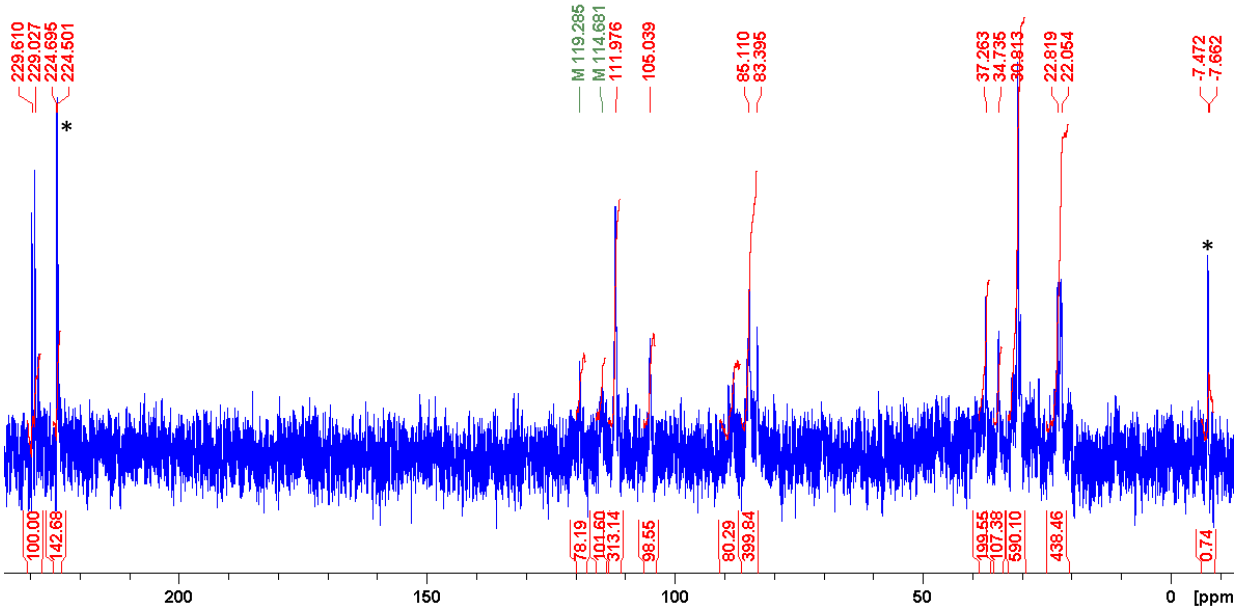

Figure S38. $^{31}P\{^1H\}$ NMR spectrum (162 MHz, C_6D_6, 298 K) of the reaction of $\mathbf{2^H}$ with dry MeOH. * is free ligand, $\mathbf{1^H}$.

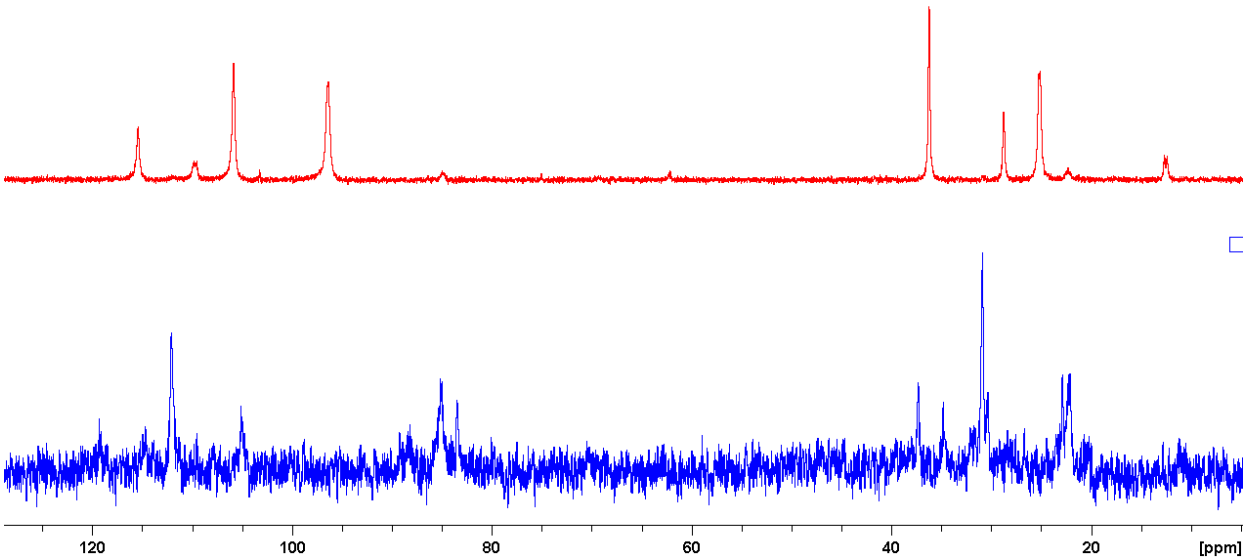

Figure S39. $^{31}P\{^1H\}$ NMR spectra (162 MHz, C_6D_6, 298 K) comparing the reaction of $\mathbf{2^{TMS}}$ (top) and $\mathbf{2^H}$ (bottom) with dry MeOH.

2.8 Reactions of A with MeOH

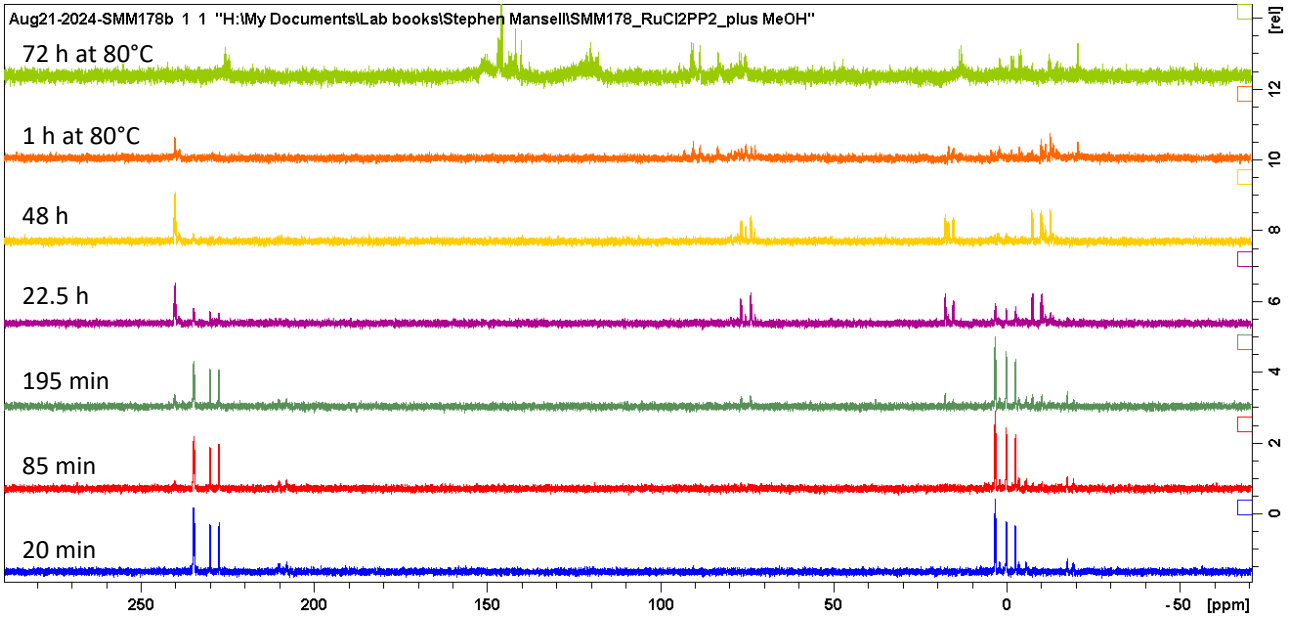

Figure S40. $^{31}P\{^{1}H\}$ NMR spectra (162 MHz, C_6D_6, 298 K) of the reaction of MeOH with **A** with time.

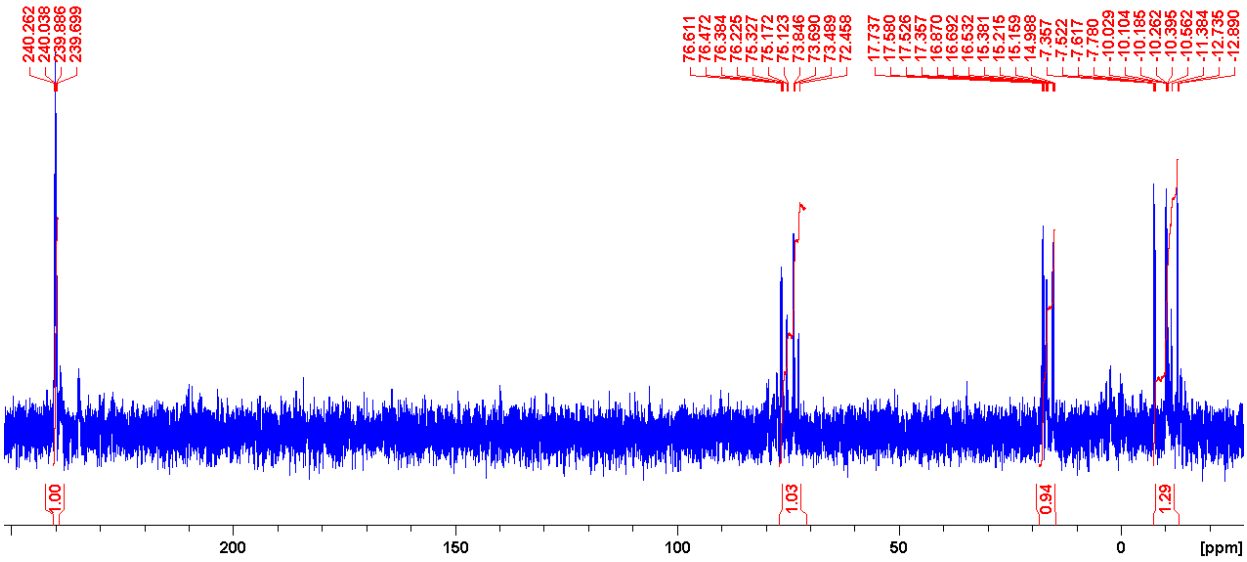

Figure S41. $^{31}P\{^{1}H\}$ NMR spectrum (162 MHz, C_6D_6, 298 K) of the product from the reaction of MeOH with **A** after 48 h at r.t.

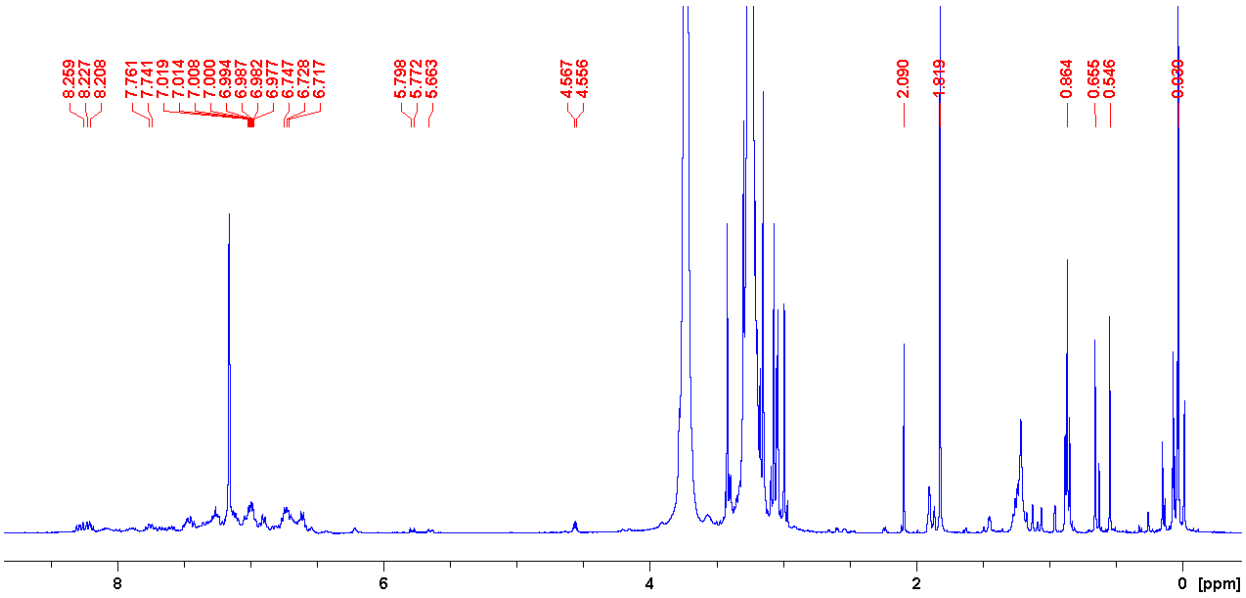

Figure S42. ^{1}H NMR spectrum (400 MHz, C_6D_6, 298 K) of the product from the reaction of MeOH with **A** after 48 h at r.t.

3 X-ray crystallography

3.1 Crystallographic details

Single crystals suitable for X-ray diffraction were covered in inert oil and placed under the cold stream of a Bruker D8 Venture diffractometer at 100 K. Exposures were collected using Cu- K_α radiation (λ = 1.54178). Indexing, data collection and absorption corrections were performed. The structures were then solved using SHELXT[1] and refined by full-matrix least-squares refinement (SHELXL)[1] interfaced with the programme OLEX2.[2] **2^{TMS}** was crystallised from a mixture of n-hexane and toluene at -25°C. ***syn*-3^{TMS}** was crystallised from a CH_2Cl_2 solution layered with pentane at -25°C. ***syn*-3^{TMS}·MeOH** was crystallised from MeOH at -25°C. ***1,4*-4^{TMS}** crystallised from a C_6D_6 solution.

The structure of **2^{TMS}** contained one molecule of toluene and one of n-hexane in the asymmetric unit, which were modelled satisfactorily but with slightly elongated thermal ellipsoids. Br2 was found to be disordered over two positions, with occupancies of 0.89:0.11. Hence, only one position of the CO ligand that must also be disordered could be located. The structure of ***syn*-3^{TMS}·MeOH** showed the MeOH molecule to sit over two positions (the carbon atom location was the same) with an occupancy of 0.86:0.14. The structure of ***syn*-3^{TMS}** was refined as a two-component twin (0.551(3):0.449(3)). For ***1,4*-4^{TMS}**, the H atoms on the functionalised phosphinine ring were freely refined (U_{iso} was constrained to 1.2 x that of the atom they are attached to) to verify their positions.

CCDC deposition numbers: 2365932-2365934 and 2380027.

3.2 Structures of additional complexes

3.2.1 Second molecule of 2^{TMS} in asymmetric unit

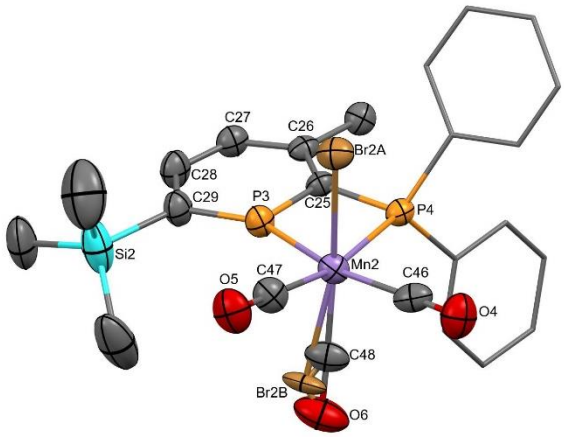

Figure S43. Molecular structure of 2nd molecule in the asymmetric unit of **2^{TMS}**. Thermal ellipsoids at 50% probability except Ph groups which are displayed as capped sticks. All H atoms except two have been removed for clarity. The Br was found to be disordered over two positions.

3.2.2 *syn*-3^{TMS}

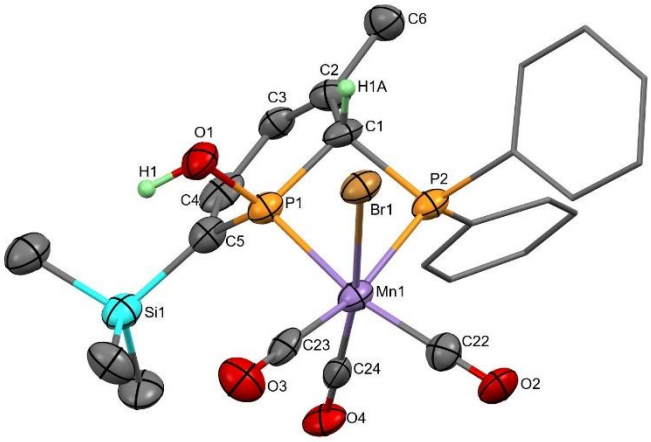

Figure S44. Molecular structure of ***syn*-3^{TMS}**. Thermal ellipsoids at 50% probability and all H atoms except two have been removed for clarity.

4.1 Crystallographic tables of data

Table S1. Additional crystallographic data.

	2^{TMS}	***syn*-3^{TMS}·MeOH**	***syn*-3^{TMS}**	***1,4*-4^{TMS}**
Empirical formula	$C_{58}H_{63}Br_2Mn_2O_6P_4Si_2$	$C_{25}H_{30}BrMnO_5P_2Si$	$C_{24}H_{26}BrMnO_4P_2Si$	$C_{31}H_{28}BrD_6MnO_4P_2Si$
Formula weight	1305.84	635.37	603.33	701.50
T/K	111.0	107.0	100.0	101.0
Crystal system	monoclinic	monoclinic	triclinic	triclinic
Space group	*C*2/*c*	$P2_1/n$	*P*-1	*P*-1
a/Å	46.5632(9)	14.2627(3)	9.1873(8)	10.7367(2)
b/Å	14.5689(3)	13.7362(3)	11.3280(11)	11.6030(2)
c/Å	19.2839(3)	14.3867(3)	13.6859(11)	13.8932(3)
α/°	90	90	73.526(6)	69.5110(10)
β/°	111.7600(10)	95.7740(10)	73.880(6)	83.7750(10)
γ/°	90	90	87.503(7)	80.4240(10)
Volume/Å^3	12149.6(4)	2804.27(10)	1311.2(2)	1596.34(5)
Z	8	4	2	2
ρ_{calc}g/cm^3	1.428	1.505	1.528	1.459
μ/mm^1	6.673	7.263	7.706	6.409
F(000)	5336.0	1296.0	612.0	712.0
Crystal size/mm^3	0.18 × 0.10 × 0.04	0.36 × 0.24 × 0.12	0.16 × 0.08 × 0.02	0.15 × 0.15 × 0.05
Radiation	CuK_α (λ = 1.54178)	CuK_α (λ = 1.54178)	CuK_α (λ = 1.54178)	CuKα (λ = 1.54178)
2Θ range for data collection/°	6.402 to 140.13	8.32 to 144.45	7.01 to 128.6	6.802 to 145.186
Index ranges	-56 ≤ h ≤ 50, -17 ≤ k ≤ 17, -23 ≤ l ≤ 23	-17 ≤ h ≤ 17, -15 ≤ k ≤ 16, -17 ≤ l ≤ 17	-10 ≤ h ≤ 10, -12 ≤ k ≤ 13, 0 ≤ l ≤ 15	-12 ≤ h ≤ 13, -14 ≤ k ≤ 14, -17 ≤ l ≤ 17
Reflections collected	104426	55731	4238	42593
Independent reflections	11534 [R_{int} = 0.0861, R_{sigma} = 0.0402]	5514 [R_{int} = 0.0393, R_{sigma} = 0.0203]	4238 [R_{int} = N/A, R_{sigma} = 0.0792]	6261 [R_{int} = 0.0425, R_{sigma} = 0.0304]
Data/ restraints/ parameters	11534/2/687	5514/1/326	4238/1/307	6261/0/375
Goodness-of-fit on F^2	1.028	1.050	1.077	1.065
Final R indexes [I>=2σ (I)]	R_1 = 0.0604, $_wR_2$ = 0.1408	R_1 = 0.0268, $_wR_2$ = 0.0677	R_1 = 0.0900, $_wR_2$ = 0.2217	R_1 = 0.0286, $_wR_2$ = 0.0758
Final R indexes [all data]	R_1 = 0.0815, $_wR_2$ = 0.1545	R_1 = 0.0280, $_wR_2$ = 0.0685	R_1 = 0.1157, $_wR_2$ = 0.2492	R_1 = 0.0300, $_wR_2$ = 0.0763
Largest diff. peak/hole (e Å^{-3})	0.95/-0.75	0.42/-0.52	1.21/-1.13	0.54/-0.46
CSD deposition numbers	2365932	2365933	2365934	2380027

5 Methanol/Ethanol Upgrading to Isobutanol

5.1 Example GC chromatograph from catalyst 2^{TMS}

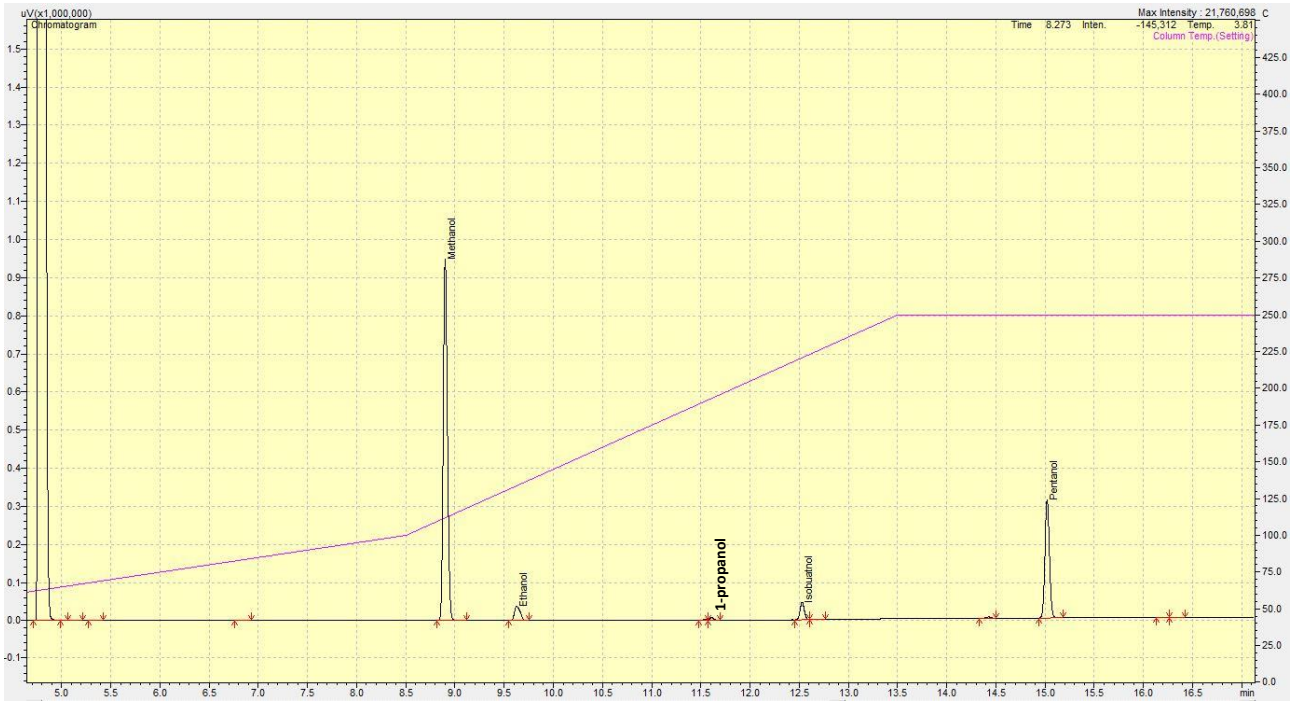

Figure S45. GC-FID chromatograph of methanol/ethanol upgrading reaction using catalyst $\mathbf{2^{TMS}}$; pentanol is the internal standard.

5.2 Example GC chromatograph from catalyst 2^{H}

Figure S46. GC-FID chromatograph of methanol/ethanol upgrading reaction using catalyst $\mathbf{2^{H}}$; pentanol is the internal standard.

5.3 Example GC chromatograph from catalyst 5

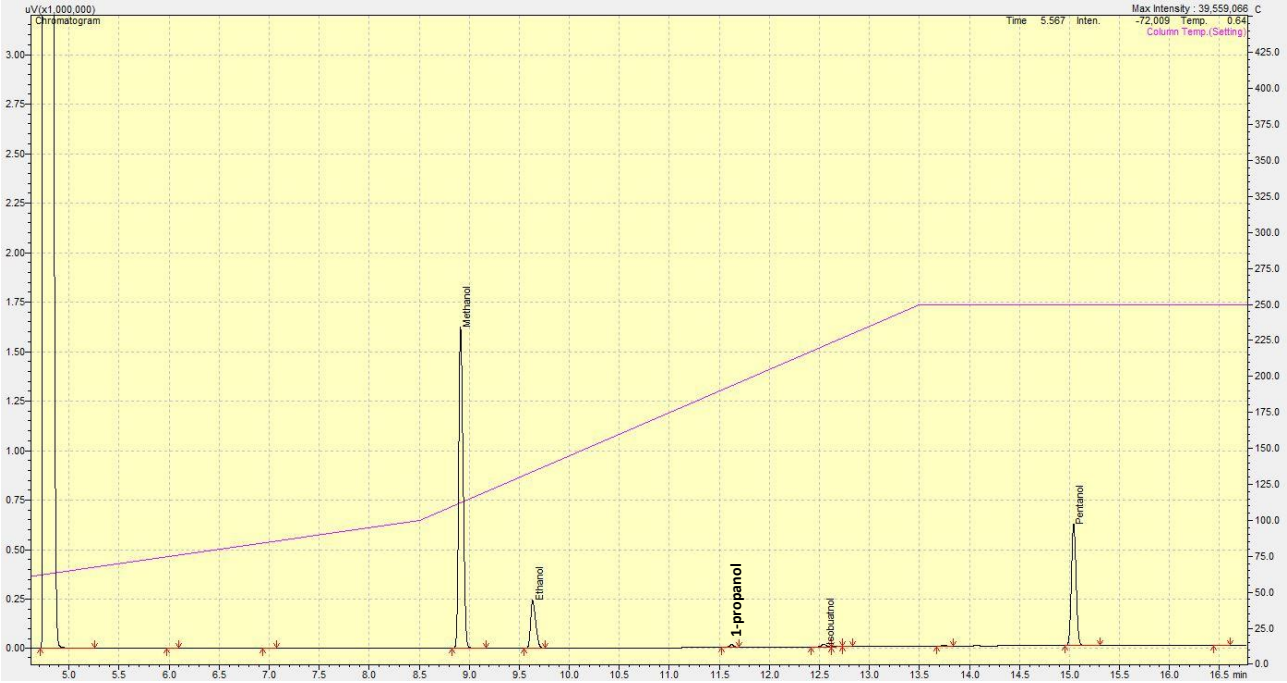

Figure S47. GC-FID chromatograph of methanol/ethanol upgrading reaction using catalyst **5**; pentanol is the internal standard.

5.4 Analysis of the solids from the Guerbet reaction

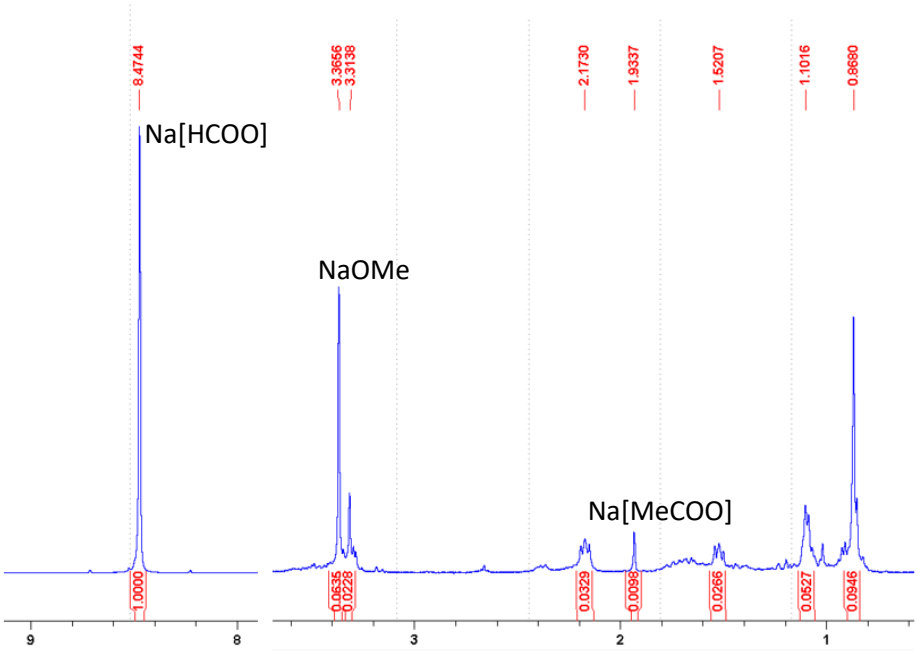

Figure S48. ^{1}H NMR spectrum (400 MHz, D_2O, 298 K) of the solids from Guerbet EtOH/MeOH upgrading to isopropanol. Section of the spectrum on the right-hand side has been zoomed in for clarity. Major product is sodium formate (peak at 8.47 ppm).[3] The peak at 3.366 is sodium methoxide and sodium acetate is at 1.93 ppm.[3]

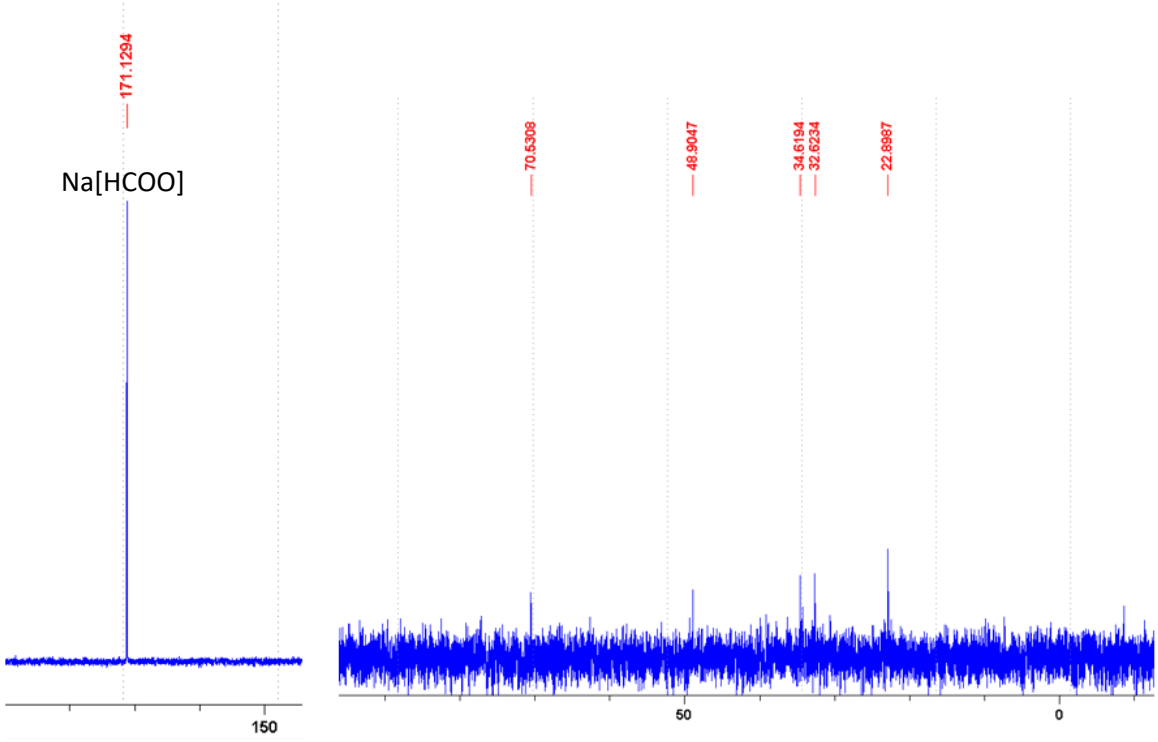

Figure S49. $^{13}C\{^{1}H\}$ NMR (101 MHz, D_2O, 298 K) spectrum of the solids from Guerbet EtOH/MeOH upgrading to isopropanol. Major product is sodium formate.[3]

6 References

1. G. Sheldrick, *Acta Crystallogr. A*, 2015, **71**, 3-8.
2. O. V. Dolomanov, L. J. Bourhis, R. J. Gildea, J. A. K. Howard and H. Puschmann, *J. Appl. Crystallogr.*, 2009, **42**, 339-341.
3. A. M. King, H. A. Sparkes, R. L. Wingad and D. F. Wass, *Organometallics*, 2020, **39**, 3873-3878.